International Journal of Pharmaceutics 418 (2011) 318–333

Contents lists available at ScienceDirect

International Journal of Pharmaceutics

journal homepage: www.elsevier.com/locate/ijpharm

Predicting solution aggregation rates for therapeutic proteins: Approaches and challenges

Christopher J. Roberts[a,*], Tapan K. Das[b], Erinc Sahin[a]

[a] Department of Chemical Engineering and Center for Molecular and Engineering Thermodynamics, University of Delaware, Newark, DE 19716, United States
[b] Biotherapeutics Research and Development, Pfizer, Inc., Chesterfield, MO 63017, United States

ARTICLE INFO

Article history:
Received 13 January 2011
Received in revised form 17 March 2011
Accepted 24 March 2011
Available online 8 April 2011

Keywords:
Protein stability
Non-native aggregation
Modeling
Biotechnology

ABSTRACT

Non-native aggregation is a common concern during therapeutic protein product development and manufacturing, particularly for liquid dosage forms. Because aggregates are often net irreversible under the conditions that they form, controlling aggregate levels requires control of aggregation rates across a range of solution conditions. Rational design of product formulation(s) would therefore benefit greatly from methods to accurately predict aggregation rates. This article focuses on the principles underlying current rate-prediction approaches for non-native aggregation, the limitations and strengths of different approaches, and illustrative examples from the authors' laboratories. The analysis highlights a number of reasons why accurate prediction of aggregation rates remains an outstanding challenge, and suggests some of the important areas for research to ultimately enable improved predictive capabilities in the future.

1. Introduction

Control of protein aggregation is a ubiquitous concern during purification, formulation, and manufacture of therapeutic protein products (Das and Nema, 2008; Mahler et al., 2009; Wang, 2005; Wang and Roberts, 2010; Weiss et al., 2009). Non-native aggregates, hereafter referred to simply as aggregates, are typically net irreversible under the conditions they form. As such, the kinetics or rates of aggregate formation are of primary interest, as these determine aggregate levels over a given period of time in different physical environments, protein concentrations, and temperatures experienced by a protein throughout its processing, shipping, and storage.

At a minimum, aggregates represent a process impurity and/or degradation product that must be controlled at relatively low levels throughout manufacture and during product storage (Cleland et al., 1993). Recent concerns have also been raised regarding the potential immunogenicity of aggregates, particularly those that are composed of multiple folded or partially folded monomers; although the precise mechanism(s) that make a particular aggregate size, morphology, and/or structure more or less immunogenic remains uncertain (Filipe et al., 2010). As such, it is also of interest to differentiate between rates of formation for aggregates ranging from small oligomers to soluble high molecular-weight (HMW) aggregates and larger, effectively insoluble particles.

In this context, the term soluble denotes species that are molecularly dispersed in solution, while insoluble is used here to denote aggregates that have coalesced into a macro- or micro-phase separated domains or particles, as it has also been shown recently that protein aggregates can reversibly transition between soluble and "insoluble" or "condensed" states (Brummitt et al., 2011a,b; Kroetsch et al., unpublished). Alternatively, one can usefully differentiate aggregates based on some measure of size and the analytical methods relevant to different size ranges (Mahler et al., 2009; Sharma and Kalonia, 2010). The former is utilized in this review, as aggregate solubility is more straightforward than the physical dimensions of an aggregate to relate to rates of monomer loss (Roberts, 2007).

Assuming aggregation is the fastest degradation route, product shelf life and the effective rate coefficient of monomer loss (k_{obs}) are then equivalent quantities when one is concerned with relatively low percent conversion of monomer to aggregate (< approx. 10%) (Weiss et al., 2009). As such, aggregation rates, shelf life, and k_{obs} are used interchangeably throughout this review. A primary goal of this review is to summarize the principles, strengths, and weaknesses of a number of different approaches to predict aggregation rates – either qualitatively or quantitatively – as a function of protein sequence/structure and solution environment. It is not practical within space constraints to exhaustively review all experimental examples or possible approaches. To the extent possible, illustrative examples from the authors' laboratories are included here to

* Corresponding author at: 223 Colburn Laboratory, 150 Academy St., Newark, DE 19716, USA. Tel.: +1 302 831 0838; fax: +1 302 831 1048.
E-mail address: cjr@udel.edu (C.J. Roberts).

0378-5173/$ – see front matter © 2011 Elsevier B.V. All rights reserved.
doi:10.1016/j.ijpharm.2011.03.064

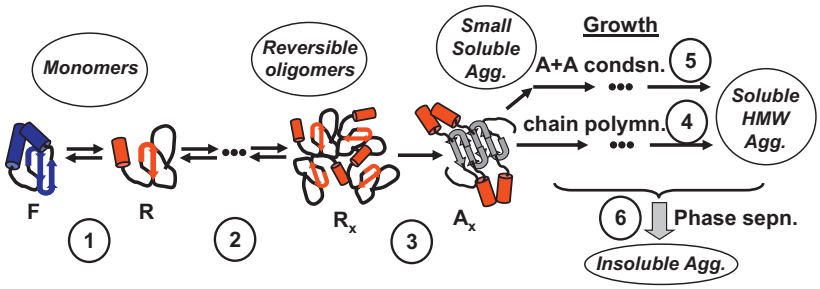

Fig. 1. Schematic representation of some of the key steps in non-native aggregation, some of which are the primary focus of different approaches to predicting relative rates of aggregation. Adapted from Li et al. (2010)..

highlight some of the key conclusions and principles throughout the report.

In what follows below, aggregation pathways are briefly reviewed in terms of features that appear to be common across a wide range of proteins. General classifications or categories of current approaches for predicting aggregation rates are then presented, followed by an outline of the organization and scope of the remainder of the article.

1.1. Overview of aggregation pathways

Assuming one is starting with a system predominantly composed of native or folded monomeric protein, aggregation at least putatively involves some or all of the following steps, depending on the size and/or solubility of the resulting aggregates (Roberts, 2007): (1) some degree of unfolding of monomeric protein; (2) reversible self association of folded or (partially) unfolded monomers; (3) structural or conformational rearrangement within otherwise reversible oligomers, so as to form key stabilizing inter-protein contacts that make the resulting aggregate nucleus net irreversible; (4) growth of nuclei or other pre-existing aggregates via monomer addition; (5) growth of aggregates via aggregate–aggregate coalescence to form larger soluble (molecularly dispersed) aggregates; (6) or growth via phase-separation to form insoluble aggregates. Fig. 1 is adapted from Li et al. (2010) and schematically illustrates the interplay between each of stages (1) to (6) as described above.

A number of important consequences follow from multi-stage aggregation pathways such as that depicted in Fig. 1. Because aggregation involves multiple stages and a number of these occur in parallel rather than in sequence, the measured rates of aggregation can depend on more than one rate-limiting step simultaneously, and can depend on what quantity or quantities are being monitored experimentally. An example of the former feature is that monomer loss depends not only on the rate of nucleation of new aggregates, but also on the rate of aggregate growth via monomer addition, and/or on the rate of aggregate coalescence if aggregates remain soluble—however, it depends primarily on nucleation rates if the resulting aggregates are insoluble (Roberts, 2007). Concerns over the method(s) used to monitor aggregation are exemplified by errors and ambiguities in aggregation rates when assays are used that are only able to detect large/insoluble aggregates – e.g., optical density or visual inspection (Morris et al., 2008; Lee et al., 2007a; Roberts, 2007) – or only aggregates that have a specific underlying secondary structure that binds a particular ligand or dye molecule. This is not to dismiss the utility of such assays for qualitative and semi-quantitative product quality assessments, but rather to highlight the need for alternatives or orthogonal metrics or validation if one wishes to accurately quantify aggregation rates in an unambiguous manner.

Although the above concerns are often overlooked by some researchers, the limitations of such assays are now reasonably well appreciated in the literature regarding pharmaceutical product development. As a result, the most common approach to quantify aggregation rates is to monitor changes in concentration (w/v basis) for monomers, small oligomers, and higher molecular weight soluble aggregates – most commonly via size-exclusion chromatography, although there is increasing interest in using alternative approaches (Gabrielson et al., 2006; Goetz et al., 2004; He et al., 2010; Liu et al., 2006). Quantifying aggregation rates in an unambiguous way for systems in which visible particles form with seemingly negligible loss of protein mass from solution remains an outstanding challenge, although subvisible particulate testing by light obscuration is a mandatory test in stability assessment of clinical supplies of therapeutic proteins, as is visual inspection (Das and Nema, 2008). In the remainder of this review, aggregation rates (ν_{agg}) will be quantified in terms of the mass fraction of protein that has been converted to aggregate of some type. The mass fraction of total protein that is monomer is denoted as m, while the fraction that exists as soluble or insoluble aggregates is then $1-m$. Aggregation rates can then be expressed equivalently in terms of k_{obs} for a given total protein concentration (c_0), solvent condition, temperature (T) and pressure (p) by

$$\nu_{agg} = -\frac{dm}{dt} = k_{obs} m^{\alpha} \quad (1)$$

with t denoting the incubation time for a given sample, and α the effective reaction order. For most pharmaceutical applications, m will be close to one, and therefore Eq. (1) can be solved for any physically reasonable value of α to give $\nu_{agg} \approx k_{obs}$. In what follows, ν_{agg} and k_{obs} are therefore used interchangeably and have units of inverse time.

It follows from Fig. 1 that there are multiple factors that contribute to k_{obs}. At a minimum, k_{obs} involves contributions from the process(es) of unfolding. More generally, aggregation rates may have contributions from unfolding, "weak" self-association, and formation of "strong" inter-protein contacts via structural motifs such as inter-protein beta sheets. As explained in more detail in subsequent sections, many common approaches to qualitatively or quantitatively predict aggregation rates can be categorized based on which of these contributions they attempt to capture. Although not shown explicitly in Fig. 1, not all of the "reactions" necessarily need occur in bulk solution. In addition to changes in solution conditions such as pH, ionic strength, and excipient concentrations, the interaction of proteins with bulk interfaces can in principle affect one or more stages in Fig. 1 (Wang and Roberts, 2010). Much of the physics that are discussed below are relevant in both cases, with additional considerations discussed briefly in the final section with regards to the potential importance of protein adsorption to bulk interfaces.

1.2. Organization and scope

Sec. 2–4 summarize the underlying principles behind different qualitative and semi-quantitative approaches to stability prediction based on the different stages in Fig. 1. Sec. 5 focuses more specifically on the question of quantitative rate prediction, highlighting a number of outstanding challenges that make this one of the long-standing problems in the field. Also included is a brief discussion of practical aspects, advantages, and limitations of different approaches. Where possible within space constraints, illustrative examples are provided from the literature to highlight the level of prediction – or lack thereof – that available approaches can currently provide.

2. Structural–conformational stability and perturbations

2.1. Underlying principles

At extremes of T and p near or above the midpoint unfolding temperature or pressure, unfolding is often found to be a rate-limiting step for aggregation (Sanchez-Ruiz et al., 1988; Kendrick et al., 1998). At more moderate conditions, ν_{agg} is expected to be significantly slower than rates of refolding, and therefore the thermodynamics rather than the kinetics of unfolding are instead expected to contribute to k_{obs} (Roberts et al., 2003; Roberts, 2007; Weiss et al., 2009). Qualitatively, this follows because the thermodynamics of stage (1) in Fig. 1 then dictate what fraction of the total monomer population exist in an aggregation-prone or "reactive" state R at a given moment in time. Thus, the greater the free energy of unfolding (ΔG_{un}) to form R monomers from folded monomers, the lower the concentration [R], and therefore the lower the rate of aggregation.

There are a multiple approaches to experimentally determining ΔG_{un}, almost all of which involve changing the sample conditions of T, p, and/or chemical denaturant concentration so as to shift the folded–unfolded equilibrium towards the unfolded state(s). The shift from folded to unfolded state(s) is then monitored spectroscopically or calorimetrically (Marky and Breslauer, 1987; Privalov, 1979, 1982). If the unfolding transition(s) can be traversed reversibly and slowly enough to allow equilibrium to be achieved throughout the transition, then ΔG_{un} can be determined and extrapolated back to the folding-favoring conditions that are typically of most interest for therapeutic protein products and protein manufacturing. To a first approximation, the temperature at which $\Delta G_{un} = 0$ for a given folding–unfolding transition is that for the corresponding local maximum in differential scanning calorimetry (DSC), or that for the midpoint between plateau spectroscopic signals. This temperature is denoted by T_M for each transition. For reasons discussed below, T_M is often only an approximate location for $\Delta G_{un} = 0$. This notwithstanding, increasing T_M then corresponds roughly to an increase in ΔG_{un} for a given unfolding transition; and therefore corresponds to a smaller population of the relevant unfolded species at a given T below T_M.

2.2. Thermal unfolding: thermodynamics and kinetics near T_M

In practice, achieving equilibrium during chemically or thermally promoted unfolding is not necessarily possible, because populating unfolded state(s) increases the rate of aggregation for aggregation-prone proteins. As most therapeutic proteins are aggregation-prone via at least some of their partially or fully unfolded conformational states, it is unusual to be able to measure robust values of ΔG_{un}, or to measure values of T_M that reflect only the unfolding thermodynamics (Remmele, 2005). To further complicate the analysis, multi-domain proteins often have multiple unfolding transitions and it is not always possible for experimental techniques to deconvolute multiple unfolding transitions (Flaugh et al., 2005a,b; Freire et al., 1992). In addition, for multi-domain proteins it is likely that only a relatively small fraction of the protein sequence is aggregation prone (see also Sec. 4). Therefore, increasing or decreasing the unfolding free energy for a given domain may have no effect on aggregation rates if that domain is not involved in forming key inter-protein contacts in the aggregates.

The above complications notwithstanding, if one is considering an unfolding transition that populates aggregation-prone monomers, T_M for that transition can still be at least qualitatively useful in predicting relative aggregation rates for a given protein as a function of solvent conditions (e.g., pH and excipient concentrations). This follows because as aggregation proceeds during thermal unfolding, the aggregation-prone or reactive (R) monomer population is continuously being depleted as monomers convert to aggregates. However, by Le Chatelier's principle the depletion of R monomers shifts the F–R equilibrium in Fig. 1 towards R, and thus the "midpoint" temperature at which approximately fifty percent of the protein has been converted from F monomers to either unfolded or aggregated protein (i.e., T_M) shifts to lower values (Sanchez-Ruiz, 1992). As a result, solution conditions that have lower T_M values for the transition that exposes aggregation-prone sequences tend to at least qualitatively correlate with higher aggregation rates at T less than approximately T_M.

Given that it is not known *a priori* which unfolding transition(s) correspond to the region(s) of a protein that is(are) aggregation prone, there remains the question of how to know which T_M value(s) are potentially relevant for predicting relative aggregation rates at lower temperatures. There are a number of approaches that have shown some level of success in this regard. One is to take advantage of the fact that unfolding transitions will show a pronounced dependence on thermal scan rate if aggregation is convoluting with unfolding during DSC scans, and T_M will shift to higher values with increasing scan rate; however, this can be misleading since T_M values also shift in this manner if the scan rate is too fast compared to folding–unfolding rates in the absence of aggregation (Lepock et al., 1992). Another is to assess the reversibility of a given unfolding transition via heating partially or completely through the unfolding transition, and assess the extent of re-folding via subsequent reheating of the same sample(s) in DSC (Remmele et al., 1999; Sahin et al., 2010). As noted earlier, in practice most unfolding transitions during thermal scanning are net irreversible if they populate aggregation-prone conformers. Thus reversibility (or lack thereof) may inform whether a given endotherm is related to aggregation. It does not, however, also assure that T_M alone will be indicative of relative aggregation rates (see also Sec. 5), as a lack of reversibility can be due to other factors—e.g., slow refolding, sample misfolding without aggregation, or lack of a chaperone needed for proper refolding from a fully unfolded state.

Alternatively, one can simply monitor aggregation chromatographically for samples that have been thermally scanned to different temperatures, and directly align the unfolding transition(s) with the loss of monomer (Sahin et al., 2010; Brummitt et al., 2011a). An example is shown in Fig. 2 for an IgG1 antibody (Sahin et al., 2010). Fig. 2 shows the overlay of a DSC thermogram (apparent heat capacity vs. T) with the corresponding monomer loss profile as a function of T, where the thermal scan rate is matched between the two experiments. The lower-T_M endotherm does not populate aggregation-prone (partially) unfolded species, and is reversible upon repeated heating and cooling through just that transition. The higher-T_M endotherm populates aggregation-prone monomers, and it is the T_M for this transition that is reasonably predictive of aggregation rates as a function of solution conditions for this antibody (Sahin et al., 2010) (see also, Sec. 5).

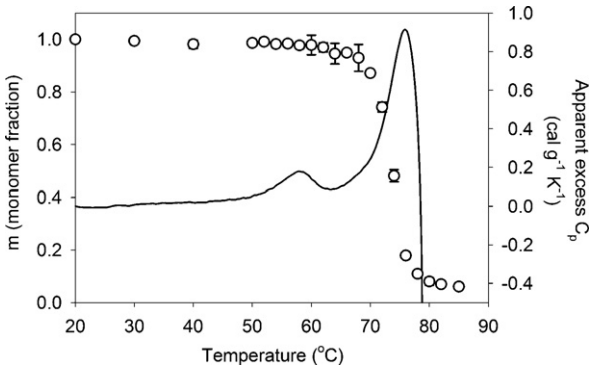

Fig. 2. Overlay of DSC thermogram (solid curve) and corresponding monomer concentration from SEC (symbols) for an IgG1 antibody during thermal scanning. The downturn in monomer concentration corresponds to the onset of the higher-T_M unfolding event(s). Adapted from Sahin et al. (2010).

The illustration in Fig. 2 helps to highlight at least one major limitation of T_M-based approaches; when one deals with multi-domain proteins there are typically multiple T_M values—i.e., multiple peaks and/or peaks with shoulders that indicate multiple unfolding transitions. As noted above, how can one know *a priori* which transition corresponds to unfolding of the aggregation-prone domain(s)? Furthermore, changes in solution conditions do not always affect all thermal transitions in the same way for a given protein. Thus, approaches based on T_M alone are often inconclusive even if one is interested only in qualitatively ranking formulation conditions. Similarly, candidate selection and optimization of protein sequence to minimize aggregation rates should not rely solely on T_M or similar approaches (see also, Sec. 5). Supplementing T_M-based measurements with thermal-scanning monomer-loss experiments such as in Fig. 2 can help to alleviate this problem, but such an approach has only been shown recently (Sahin et al., 2010; Brummitt et al., 2011a).

2.3. Structural perturbations far from T_M

The same mechanistic reasoning that underlies T_M-based approaches to qualitatively predict (i.e., to rank) aggregation rates for a given protein also motivates approaches based on screening formulation conditions for those that minimize structural perturbations to the folded state at the target storage temperature of interest. That is, if a particular choice of solution conditions leads to a detectable structural perturbation of the otherwise folded monomer species then this potentially exposes aggregation-prone polypeptide sequences or regions of the protein. This is a potentially attractive approach in that it allows one to focus on lower temperatures (e.g., room temperature) and short time scales (e.g., hours to days to weeks) for the experimental screening conditions.

The major shortcomings of this approach are at least two-fold. The first is similar to that noted above for T_M-based approaches: if one does not know *a priori* what region of the protein is aggregation prone, how can one deduce whether a detected structural perturbation is relevant from the perspective of populating aggregation-prone monomers? If one must take the time to measure aggregation rates under "real-time" storage conditions in order to confirm that a structural change was relevant, then this defeats the purpose of "predicting" rates from a structural perturbation approach; although the knowledge that such structural changes correlate with aggregation may still be useful from a pedagogical and qualitative mechanistic point of view (Raso et al., 2005). However, in order to be truly predictive in a practical sense, one needs a way to know which structural changes are relevant to aggregation, and then also to be able to measure those changes unambiguously; this remains an open challenge and active area of research (cf., Sec. 4 and 5).

The second major shortcoming of structural-perturbation approaches is the limitation of available techniques to probe perturbations that are either rare or too short-lived to be detectable. Experimentally, circular dichroism (CD), intrinsic/extrinsic fluorescence (FL), infrared (IR) or other spectroscopies are commonly used to detect structural perturbations (Weiss et al., 2009). However, none of these techniques will likely be able to detect a structurally perturbed species (unless largely unfolded) that populates less than approximately 1–10 percent of the total protein population, depending the degree of structural perturbation and/or sensitivity of the technique. Thus, it is fundamentally incorrect to conclude generally that a lack of detectable difference in a population-averaged spectrum is evidence that a change in formulation condition does not significantly alter the population of partially or fully unfolded monomers (Roberts, 2007); similarly, one cannot argue that lying far below T_M means that the population of (partially) unfolded monomers is zero or negligible– it may simply be below the detection limit(s) for the assay of interest. Certain assays are more sensitive to small or local perturbations – e.g., intrinsic/extrinsic fluorescence – and so may be able to extend the detection thresholds to lower (but still finite) limits (Maas et al., 2007; Demeule et al., 2009; Gabellieri and Strambini, 2006).

As an example, if a change in formulation condition or protein sequence causes the concentration of R monomers to increase from 0.001% to 0.01% this will be experimentally undetectable for practical purposes. However, the concentration of "reactants" has changed by an order of magnitude and the rate of aggregation would then change by this amount or more, depending on the effective reaction order. This is the expected situation on general thermodynamic grounds whenever one operates at temperatures well below T_M, as the total concentration of R monomers will be much smaller than that of the fully folded species (Roberts, 2007). As a result, approaches that rely on structural perturbations far from T_M may be useful in eliminating some of the most aggregation-prone conditions. However, they may be of little use in discriminating between different conditions that are all reasonably stable on the time scale of days to weeks, but have significantly different aggregation rates when measured on month to year time scales. Even if one is able to identify more sensitive techniques for detection of structural perturbations, this does not assure those perturbations populate aggregation-prone species and will be indicative of relative aggregation rates upon storage.

3. "Weak/reversible" protein–protein interactions

3.1. Underlying principles

All molecules in a solution interact with their neighbors; at a minimum these are so-called steric repulsions that are present for all real molecules. In addition to steric repulsions, all molecules experience London dispersion or van der Waals (vdW) attractions to some degree. The remaining interactions that are significant for most aqueous solutions are hydrogen bonding (attractions), hydrophobically driven attractions, and electrostatic attractions and repulsions (Israelachvili, 1991).

Protein–protein interactions in solution can typically be grouped into two categories: "strong" interactions that result in specific "binding" between monomers that compose native multimers such as trans-thyretin (Palaninathan et al., 2008) and arc-repressor (Robinson et al., 1997); and relatively "weak" or non-specific, colloidal interactions that influence the local concentration of protein in solution (Weiss et al., 2009; Chi et al., 2003a; Israelachvili, 1991). In this context, colloidal interactions

refer to the combination of attractive and repulsive interactions noted above, in which there are not a small number highly specific "lock-and-key" structures that give rise to stable, native multimers. Rather, many different arrangements between two or more proteins have similar free energies, and are not separated from each other by large free energy barriers.

Although colloidal interactions are sometimes referred to within the context of oligomer formation, this may portray a false picture in which there is a definable "complex" for such self-associated states. A more useful approach may be to consider such protein–protein interactions in the context of preferential exclusion and preferential accumulation, such as that used to explain protein–cosolute interactions (Timasheff, 1993). If one considers the spatial distribution of proteins within the vicinity of a selected reference protein, protein–protein interactions that are favorable (unfavorable) relative to protein–solvent interactions result in preferential accumulation (exclusion) of proteins compared to solvent around a given reference protein.

Fig. 3 illustrates this concept with three illustrative examples of protein–protein radial distribution functions ($g_{22}(r)$) as a function of the center-to-center distance (r) between two proteins. $g_{22}(r)$ gives the local concentration of protein, divided by the bulk concentration, at a distance r from the center of a reference protein. That is, $g_{22}(r) > 1$ indicates a local protein concentration at r that is higher than the bulk concentration, and vice versa. If two proteins interact with only an effective hard-sphere (HS) or purely steric repulsion, $g_{22}(r)$ appears as in Fig. 3A, with zero probability for $r < d$ since the proteins cannot overlap, with d defined as the effective HS diameter of single protein. Preferential accumulation is illustrated by Fig. 3B, with higher local concentrations within the immediate vicinity of the central protein—i.e., for r/d between 1 and approximately 2. Preferential exclusion is illustrated in Fig. 3C, with local concentrations that are lower than the bulk concentration for r/d extending beyond the steric-repulsion distance.

3.2. 2nd Osmotic virial coefficient (B_{22})

The osmotic second virial coefficient (B_{22}) is accessible experimentally via experiments such as light or neutron scattering (Velev et al., 1998), equilibrium analytical ultracentrifugation, self-interaction chromatography (Tessier et al., 2002), and classic osmotic pressure experiments (Alford et al., 2008). B_{22} provides an integrated measure of $g_{22}(r)$ via its statistical mechanical definition (Ben Naim, 1992):

$$B_{22} = B_{22}^{HS} - \frac{1}{2}\int_{r/d=1}^{\infty} (g_{22}(r) - 1) 4\pi r^2 \, dr \qquad (2)$$

In Eq. (2), B_{22}^{HS} denotes the *HS* value for B_{22}. Rigorously, Eq. (2) is accurate only in the limit of low protein concentration (Ben Naim, 1992). If one works at high enough protein concentrations that most proteins interact closely with multiple proteins simultaneously – e.g., "crowded" conditions (Minton, 2008) – B_{22} must be replaced with the corresponding Kirkwood-Buff integral (G_{22}) that applies at any protein concentration (Ben Naim, 1992; Blanco et al., in preparation). The qualitative concepts and discussion below are independent of whether B_{22} or G_{22} is the more appropriate quantity for a given range of protein concentrations.

Eq. (2) is often represented in an equivalent form by replacing $g_{22}(r)$ with $\exp(-W_{22}(r)/k_BT)$, with $W_{22}(r)$ denoting the potential of mean force (Ben Naim, 1992; McQuarrie, 1976) or the reversible work required to bring two proteins together from infinite separation to a distance r, with all protein orientations averaged for each protein, and all solvent degrees of freedom averaged for each value of r between the two proteins. Given the discussion and definitions above in which purely steric interactions are taken as the reference state, $B_{22} > B_{22}^{HS}$ corresponds to preferential exclusion of proteins in the vicinity of each other, and vice versa for $B_{22} < B_{22}^{HS}$. In addition, the discussion above highlights that $B_{22} = B_{22}^{HS}$ may be a more appropriate reference point than $B_{22} = 0$ for delineating between net attractive versus repulsive conditions in the context of protein aggregation kinetics (Weiss et al., 2009; Sahin et al., 2010).

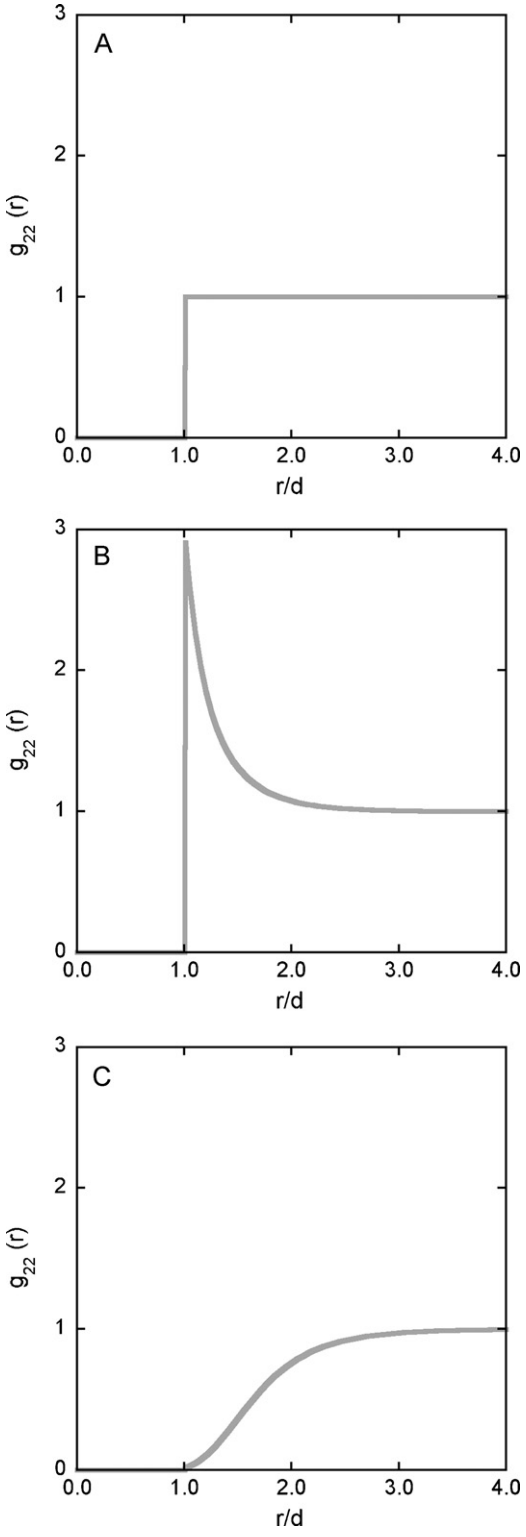

Fig. 3. Illustrative radial distribution functions $g(r)$ for a purely steric or HS repulsion (A) or for steric repulsions plus attractions (B) or non-steric repulsions (C) leading to higher or local concentrations of protein, respectively.

In the context of the above discussion, defining a reduced or dimensionless virial coefficient (b_2^*) as

$$b_2^* = \frac{B_{22}}{B_{22}^{HS}} - 1 \tag{3}$$

then gives that positive (negative) b_2^* corresponds to local protein concentrations in the vicinity of the protein surface that are lower (higher) than the bulk protein concentration. As depicted in Fig. 1, nucleation requires proteins to first approach each other closely. This is more (less) likely to occur if the local concentration of proteins is higher (lower). Therefore, conditions of positive (negative) b_2^* are expected to correspond to slower (faster) aggregation rates if all other factors are held fixed. However, in practice it may be difficult to keep those other factors fixed while altering b_2^* (see also Sec. 5).

3.3. Effective charge (Z^*)

The effective charge (Z^*) on a protein reflects the combination of its molecular or raw charge (Z) plus any territorial ions that are loosely or strongly bound to the protein surface (Chase and Laue, 2008). Z^* is the average charge that another protein "feels" as two proteins approach each other, not accounting for induced charge fluctuations that might, in principle, occur if one is near the pK_a of a given ionizable amino acid group on the protein surface (Yadav et al., 2010), and not accounting for highly asymmetric surface charge distributions (Neal et al., 1998). To a first approximation, Z^* gives an estimate of the magnitude of electrostatic repulsions between proteins. Z^* can be determined experimentally by measuring the electrophoretic mobility and tracer diffusivity in free solution (Chase and Laue, 2008; Brummitt et al., 2011b). In principle, high Z^* corresponds to strong electrostatic repulsions that enhance preferential exclusion and thereby reduce aggregation rates. Of course, protein–protein interactions include non-electrostatic contributions that may overwhelm electrostatic repulsions, and so Z^* is not a sole indicator of conditions to maximize preferential exclusion by proteins for one another.

As noted above, Z^* does not account for the spatial distribution of charges on the protein surface; if that distribution is sufficiently asymmetric then it is possible that charged regions or patches on one protein can have favorable electrostatic interactions with oppositely charged patches on another protein, resulting in net attractive protein–protein interactions despite the proteins having the same overall net charge. This situation can be identified experimentally, for example, by observing b_2^* values that are negative at low ionic strength (low degree of charge screening) but that become less negative with increasing ionic strength (Sahin et al., 2010).

Positive b_2^* values can only occur if the net electrostatic interactions between two proteins are repulsive, and therefore indicates that asymmetric, attractive charge–charge interactions are not dominant (Sahin et al., 2010). In such cases b_2^* might be reasonably approximated by modeling $W_{22}(r)$ with a screened electrostatic colloidal potential such as (Jin et al., 2006)

$$W_{22}(r)\big|_{r>d} \sim \frac{(Z^*)^2}{r/d}\ \exp\left[-\kappa d\left(\frac{r}{d}-1\right)\right] \tag{4}$$

where κ is the inverse Debye screening length and is determined by the concentration and valency of any free ions in solution (Israelachvili, 1991). Using Eqs. (2) and (3), the definition of $g_{22}(r)$ in terms of W_{22}, and the definition $B_{22}^{HS} = (2/3)\pi d^3$ one can express b_2^* in terms of W_{22} as

$$b_2^* = -3\int_{\tilde{r}=1}^{\infty} (e^{-W_{22}(\tilde{r})/k_BT} - 1)\,\tilde{r}^2\,d\tilde{r} \tag{5}$$

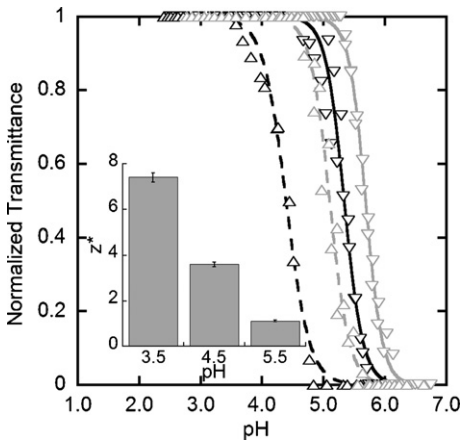

Fig. 4. Percent transmittance at 650 nm as a function of pH during titration from low to high pH (downward triangles) and upon reversal and titration from high to low pH (upward triangles) for aggregates that were created as soluble species at low pH before the titrations depicted above. Differences in the location of the gray and black symbols are putatively due to differences in the total protein concentration. Curves are empirical fits as guides to the eye. Inset shows Z^* values at selected pH values, illustrating that electrostatic repulsions are greatly reduced as the transition from soluble to insoluble aggregates is approached. From Brummitt et al. (2011b), with permission.

where $\tilde{r}$ denotes the reduced distance r/d. Comparison of Eqs. (4) and (5) shows that under conditions of strong net repulsions between proteins ($b_2^* \gg 1$) it is reasonable to expect that Z^* and b_2^* provide similar information to assess the magnitude of monomer–monomer repulsions.

3.4. Protein–protein interactions and aggregate phase behavior

The above discussion focused on protein–protein interactions from the perspective of monomer–monomer interactions. However, recent examples show that aggregate–aggregate interactions can play an important role in determining whether aggregates that form as molecular species such as dimers, oligomer, or other high-molecular-weight species will ultimately coalesce with one another to form large, visible species. A strong correlation was observed between b_2^* and conditions of pH and [NaCl] that led to soluble (molecularly dispersed) vs. insoluble (macroscopic) particles for α-chymotrypsinogen A (Li et al., 2010) as well as a series of monoclonal antibodies (Sahin et al., 2010). Conditions with strong electrostatic repulsions ($b_2^* \gg 1$) maintained soluble aggregates and limited aggregate growth, while conditions where electrostatic repulsions were sufficiently suppressed by moving to higher pH and/or higher ionic strength led ultimately to rapid coalescence of aggregates to form large visible particles (Li et al., 2010; Sahin et al., 2010).

A similar correlation was also observed for a different IgG1 antibody, where increasing pH led to decreasing b_2^* and a transition from soluble to insoluble aggregates. Fig. 4 illustrates this by showing cloud point transitions from soluble (transparent) to insoluble (hazy) solution conditions for this antibody as a function of pH (Brummitt et al., 2011b). Monomers are soluble at all pH conditions in Fig. 4, and the hysteresis loops show that the sharp transition from soluble (high percent transmission, %T) to insoluble (low %T) conditions is reversible. This example illustrates that there is a thermodynamic basis for distinguishing between conditions where aggregates are stable as molecularly dispersed (i.e., dissolved) species. As such, it appears that there is a fundamental distinction between soluble and insoluble aggregates that goes beyond semantic arguments regarding what is detectable to the naked eye. Furthermore, such results suggest that some formula-

tion conditions are inherently more prone to particle (or particulate matter) formation (Brummitt et al, 2011b; Sahin et al., unpublished). Finally, the inset in Fig. 4 shows that the transition from soluble to insoluble aggregates correlates strongly with the drop in Z^*; supporting the view that maximizing charge–charge repulsions between proteins can be beneficial by helping to prevent visible particle formation.

4. "Strong/irreversible" protein–protein interactions

The definition of irreversible and strongly associated aggregates depends on the type of assay used, and is generally based on observing undissociated aggregates under conditions where weakly-bound aggregates will disintegrate. Most commonly these are aggregates detected by SE-HPLC, SDS polyacrylamide gel electrophoresis (PAGE), analytical flow-field-flow fractionation (AFFFF), and mass spectrometry (MS). When the protein components (monomer or fragments) form aggregates, if they are cross-linked by covalent bonds it is likely that such species will be detected in SDS-PAGE and MS as well as when fractionated by SE-HPLC or AFFFF. If the aggregates form simply by strong non-covalent interactions (hydrophobic, hydrogen bonding and/or electrostatic), then it can be potentially detected by non-denaturing fractionation conditions (SE-HPLC/AFFFF).

As discussed in later sections, experimental approaches such as various stress have been applied by researchers to predict the propensity of aggregate formation. Although it is extremely challenging to predict what type of aggregates (weakly bound, strongly bound, covalent) might form from a given stress factor, it is generally recognized that formation of covalent aggregates may be induced by chemical causes such as oxidants, free radicals, and redox mediators.

Many computational approaches to predict strongly-bound (non-covalent) aggregates rely heavily on a single or a few parameters—particularly the hydrophobicity of amino acids that constitute a given protein. The underlying principle of these approaches is that hydrophobic groups attract each other and have an inherent propensity to minimize exposure of hydrophobic surface to bulk solvent (water) and other hydrophilic groups. Depending on the 3-dimensional arrangement of the constituent amino acids in a protein, such hydrophobic groups can be spatially clustered to cooperatively provide a strong enough attractive force to keep two (or more) proteins monomers "glued" together. The stability of aggregates formed by hydrophobic interactions is expected to be temperature dependent as hydrophobic interactions are strongly temperature dependent—with model systems exhibiting the greatest propensity for hydrophobic association near ambient temperature (Schellman, 1997; Rees and Robertson, 2001); the physics underlying this temperature dependence also plays a role in the observation that protein unfolding free energies and enthalpies are temperature dependent, due to its influence on the heat capacity of unfolding (see also discussion of *Non-Arrhenius Temperature Dependence* in Sec. 5).

Several approaches focused on the hydrophobicity of exposed amino acids residues have been used in predicting protein folding pathways and more recently for protein aggregation. The newer approaches (Chennamsetty et al., 2009, 2010; Wang et al., 2009) involve a combination of hydrophobicity and structural prediction, where structural prediction (using molecular simulation and homology modeling) plays a critical role in measuring the fraction of such hydrophobic residues that are exposed to solvent when dispositioned throughout the three dimensional structure of a protein. A number of published reports and approaches (Caflisch, 2006; Cellmer et al., 2007) account the role of hydrophobic interactions to predict formation of amyloid fibril or beta-sheet dominated aggregation processes in relatively small proteins, protein fragments, or synthesized polypeptides. Although hydrophobicity calculations based on amino acid sequence alone have clearly been useful to identify potentially aggregation-prone regions in polypeptides lacking substantial tertiary structure, it is not clear that such calculations will work well for larger, "foldable" proteins in which most of the aggregation prone regions are protected from exposure to solvent and (more importantly) contact with other proteins—and these are often the proteins of most therapeutic relevance. An additional and important limitation of current approaches that do account for tertiary structure at some level is that they are limited by the inherent experimental bias of crystal structure(s) towards those which crystallize. NMR structures include contributions from more than just those that are compatible with crystal formation, however they report primarily the dominant conformers in solution, and are limited in their ability to inform about relatively disordered regions. As such, the structural information from crystallography and/or NMR is not expected to reflect rare conformational fluctuations that may be most relevant to forming strong inter-protein contacts. This limitation notwithstanding, unfortunately most therapeutic proteins do not have such structures available in atomic detail; this is particularly the case for relatively large proteins such as antibodies and their conjugates.

In addition, burial and location of hydrophobic amino acids is not the only factor in some available algorithms to predict aggregation propensity. It is also balanced with the inherent beta-sheet and empirical amyloid-formation propensities of different amino acids in a number of the so-called "aggregation calculators" that are available in the public domain (Conchillo-Sole et al., 2007; Trovato et al., 2007; Fernandez-Escamilla et al., 2004; Wang et al., 2009). The few amyloid structures known to date at a molecular scale clearly indicate the importance of inter-peptide hydrogen bonding as a stabilizing motif for "irreversible" or "stable" aggregates, as well as the packing of side chains along the periphery of the resulting (highly polymerized) aggregates (Eisenberg et al., 2006; Nelson et al., 2005). While all amino acids are capable of hydrogen bonding via their amide backbone, it appears that the most aggregation prone are those that are able to form stabilizing inter- (and intra-) peptide hydrogen bonds while also protecting large "patches" of hydrophobic amino acids from solvent exposure, and providing favorable side-chain packing without large electrostatic repulsions. Interestingly, these same principles are at the core what drives protein folding (Chiti and Dobson, 2006; Laurence and Middaugh, 2010). Thus, at some level one can view the problem of prediction of (non-native) aggregation of proteins as a version of the protein-folding problem; however an arguably more complex one, in that one must allow for the pathways by which multiple proteins simultaneously "misfold", combine with one another, and find a stable inter-protein "fold" within an aggregate (Laurence and Middaugh, 2010). Presumably, advances in methods to predict the pathways for folding of larger and larger proteins (i.e., multiple polypeptide chains) will also benefit the prediction of aggregation of proteins more generally. Although methods to predict aggregation "hot spots" from knowledge of the experimental "fold" within the stabilizing core of aggregates exist (Eisenberg et al., 2006), these have been designed and validated primarily for polypeptides and small proteins thus far (Ivanova et al., 2006). While many available studies focus primarily on aggregation proceeding via conversion from native structures to non-native beta-sheet-rich structures, alternative mechanisms may also exist—notably domain-swapping to form dimers or even multi-mers that retain much of their native secondary structure but form strong non-native contacts between domains on adjacent proteins (Rousseau et al., 2003).

As noted earlier, more recent approaches (Chennamsetty et al., 2009, 2010; Wang et al., 2009) for aggregation prediction involves computationally intensive simulations of larger proteins such as

monoclonal antibodies to derive a structure that helps to calculate surface-exposed regions. Chennamsetty et al. (2010) developed a parameter they denoted as a spatial aggregation propensity (SAP) based on atomistic simulations of full antibody or fragments of the antibody to predict aggregation prone regions. This method calculates the effective, dynamically exposed hydrophobicity of a certain patch on the protein surface that is used to determine critical regions for aggregation in antibodies. The authors defined positive SAP values to correspond to hydrophobic regions or patches, with a high value of SAP indicating a highly exposed hydrophobic region, while a low value indicates a buried hydrophobic region. Larger regions of high SAP were hypothesized to correspond to regions involved in aggregate formation. The computational work was supplemented by creating experimental mutants in certain high-SAP regions by changing hydrophobic residues to hydrophilic. SE-HPLC and turbidity data of some of the mutants were reported to correlate well with SAP prediction, while some of the mutants showed enhanced aggregation contrary to prediction. It was suggested that the SAP prediction method could be used in early stages of antibody selection process improving stability.

Wang et al. (2009) used computational approaches to explore the aggregation potential of monoclonal antibodies via cross or extended β-motifs—similar to those reported for amyloid-forming proteins (Nelson et al., 2005; Jaroniec et al., 2002; Jones et al., 2003). As much of the conserved sequences of monoclonal antibodies are natively beta-sheet prone, it is possible that this predisposes them to amyloid-like structures in aggregates; however, it is not clear whether that is necessarily the case, as examples exist of natively helical proteins that form amyloid-like aggregates (Pertinhez et al., 2001; Fändrich et al., 2001; Picotti et al., 2007; Weiss et al., 2007). Such speculations notwithstanding, the analysis in Wang et al. (2009) focused on sequence-based prediction tools (TANGO and PAGE) to identify the potential aggregation-prone regions of several antibodies. It should be noted that the TANGO and PAGE methods have been parameterized using data from amyloidogenic peptides and proteins, hence these methods may have bias towards finding regions of amyloidogenic behavior. The common features among the aggregation-prone motifs found in both variable and constant domains were that they are rich in hydrophobic, aromatic or glutamine/asparagine residues (Sanchez et al., 2005; Azriel and Gazit, 2001) but relatively low in the density of charged residues. Additionally, when the aggregation-prone regions predicted from amino acid sequence were mapped on to the homology-modeled three-dimensional Fab structures, the ones in the complementary determining regions (CDRs) co-localized with the putative antigen binding site. It remains to be seen if these predicted aggregation prone regions actually correlate with any available experimental data of aggregation propensity.

As much of the discussion above highlights, prediction of actual, quantitative rates – as opposed to ranking of relative rates or correlating within an empirical data set – is not within the scope of available algorithms or models for this stage of the aggregation process. This is not surprising, as the stage(s) of aggregation that involve the structural rearrangement of multiple proteins at once is(are) arguably well beyond the limitations of even the most powerful computational resources if one is to consider the problem in atomistic detail (Choutko et al., 2011; Morra et al., 2008).

Experimentally, it is also not yet possible to directly monitor the rate(s) of conversion from reversible, "weakly bound" clusters to net irreversible, "tightly bound" aggregates (i.e., nuclei in Fig. 1). This follows because these species are too poorly populated and/or too short-lived to either be isolated easily or to be monitored directly. However, in some cases it is reasonable to examine aggregates *a posteriori* in order to identify key amino acid sequences that compose the tightly bound "core" of the aggregates. As noted above in the context of the "aggregation calculators", the predicted "hot spots" in aggregation-prone proteins are often only predictions—i.e., they are not actually verified experimentally (Wang et al., 2009).

Experimental techniques that are typically employed to identify "hot spots" of sequence or key regions/domains that help to stabilize aggregates include: incomplete proteolysis (Ignatova et al., 2007); scanning mutagenesis (Li et al., 2002); and a combination of hydrogen-deuterium exchange (HDX), mass spectrometry (MS), and aggregate dissociation plus proteolysis (Zhang et al., 2010; Tobler and Fernandez, 2002). Incomplete proteolysis works on the principle that any amino acids in (soluble) aggregates that are well protected from proteases must be buried within the core of the aggregate. Scanning mutagenesis uses exhaustive scanning of point mutations across a stretch of amino acids in order to identify which amino acid residue(s) most disrupt aggregate formation in the first place. In practical terms, such an approach is limited to relatively small proteins and polypeptides.

HDX-MS with dissociation and proteolysis is based on the following strategy (Tobler and Fernandez, 2002; Zhang et al., 2010). Pre-formed aggregates in hydrogenated solvent are first incubated with deuterated solvent for different periods of time, to allow solvent-exposed amide backbone protons to exchange with deuterium. After selected exchange times, samples are placed into acidic solutions with high concentrations of urea or guanidinium salts to simultaneously quench HDX and disrupt any non-covalent inter- and intra-protein contacts. After a short period of time to allow dissociation and unfolding of protein chains, but not long enough to allow significant HD back-exchange, samples are incompletely proteolyzed into small polypeptide fragments and analyzed with MS to quantify the number of exchanged amide protons. These fragments or reporter peptides then typically fall into one of three categories depending on their solvent exposure (i.e., their accessibility to HDX): (i) less solvent exposed in the aggregate than in the folded monomer; (ii) equally or similarly solvent exposed in the aggregate and folded monomer; (iii) more solvent exposed in the aggregate than the folded state (Tobler and Fernandez, 2002; Zhang et al., 2010).

Amino acids that fall into category (i) are interpreted to have become buried within a tightly bound "core" of inter-protein contacts. Amino acids in category (ii) could also be involved in such a "core" region, but could instead simply lie in a region of the protein that did not unfold as part of the aggregation process. As such, the role of amino acids in category (ii) remains ambiguous from this technique alone. Amino acids in category (iii) have become more exposed to solvent via aggregation, and thus are not likely to not participate in strong inter-protein contacts within aggregates. An illustrative example of the results of such as study is shown in Fig. 5 for aggregates of the globular protein α-chymotrypsinogen A (aCgn), adapted from Zhang et al. (2010).

Fig. 5 shows the FASTA sequence of aCgn numbered from N- to C-terminus. The bold red letters show the peptide sequences that are even more protected from HDX in the aggregate than they are in the folded state (i.e., category (i) above). These provide an experimental measure of the "hot spots" for aggregate formation that is independent of any computational predictions. The colored solid lines above each row of the FASTA sequence show the predictions from three public-domain "aggregation calculators". Obviously, no one calculator accurately predicts only the experimental "hot spots" as measured by HDX-MS—there are number of false positives and negatives. Interestingly, a consensus of the three calculators does reasonably well at predicting one of the hot spot peptide regions, and such a consensus approach has proven useful in identifying amino acids for replacement so as to inhibit aggregation in γ-D crystallin (Sahin et al., 2011). The inability of the calculators to robustly predict the aggregation hot spots in aCgn notwithstanding, the HDX-MS approach is promising for its ability to identify the hot

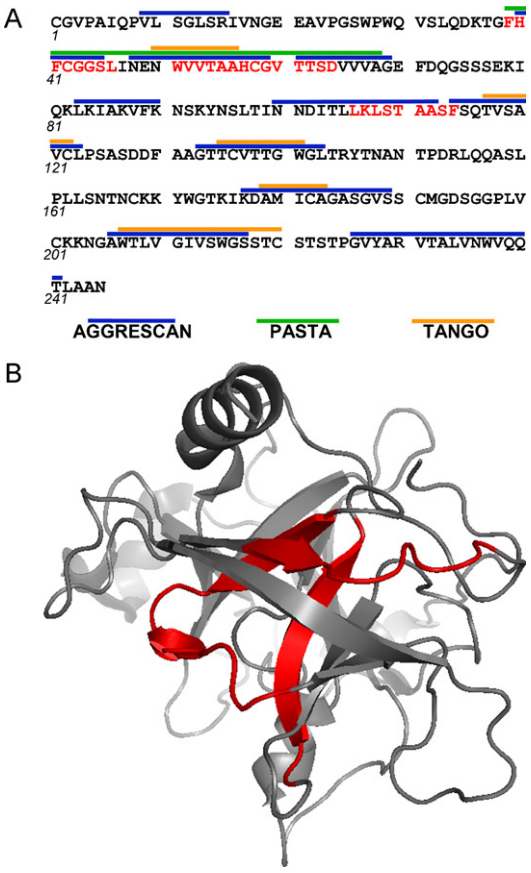

Fig. 5. (A, top) Comparison of experimental "hot spots" from HDX-MS (red bold letters) and predictions from selected "aggregation calculators" (overbars) for aggregation of aCgn; (B, bottom) X-ray crystal structure of aCgn with experimental hot spots highlighted in red to illustrate the burial of the hot spot region within the three dimensional folded structure. Adapted from Zhang et al. (2010). (For interpretation of the references to color in this figure legend, the reader is referred to the web version of the article.)

spots from a purely experimental standpoint. This may be useful in future for the rational design of proteins that have lower "reactivity" or inherent aggregation propensity, as well as for improved mechanistic modeling of the aggregation process—and ultimately improved prediction of aggregation rates.

5. Prediction of aggregation rates

5.1. T_M and relative aggregation rates

As the discussion in Sec. 2 highlighted, T_M can at least correlate with k_{obs}. A simple analysis shows why T_M alone should never be expected to be quantitatively predictive of k_{obs}, as follows. In the idealized case where the experimental T_M is the temperature at which $\Delta G_{un} = 0$ for the F–R transition in Fig. 1, ΔG_{un} as a function of temperature can be expressed thermodynamically in terms of T_M as well as the corresponding enthalpy of unfolding evaluated at T_M (denoted ΔH_0) and the heat capacity of unfolding (Δc_p) (Becktel and Schellman, 1987; Weiss et al., 2009). Provided that one is not too close to T_M, the value of k_{obs} is expected to scale exponentially with ΔG_{un} (Roberts, 2007; Weiss et al., 2009). Therefore, k_{obs} must depend on at least T_M, ΔH_0, and Δc_p—although the dependence on Δc_p may be negligible for practical purposes if one is not very far below T_M (Weiss et al., 2009).

In practice, it is often not possible to determine equilibrium unfolding values for T_M, ΔH_0, and/or Δc_p. As such, the most common practice is to simply, qualitatively rank formulations based on

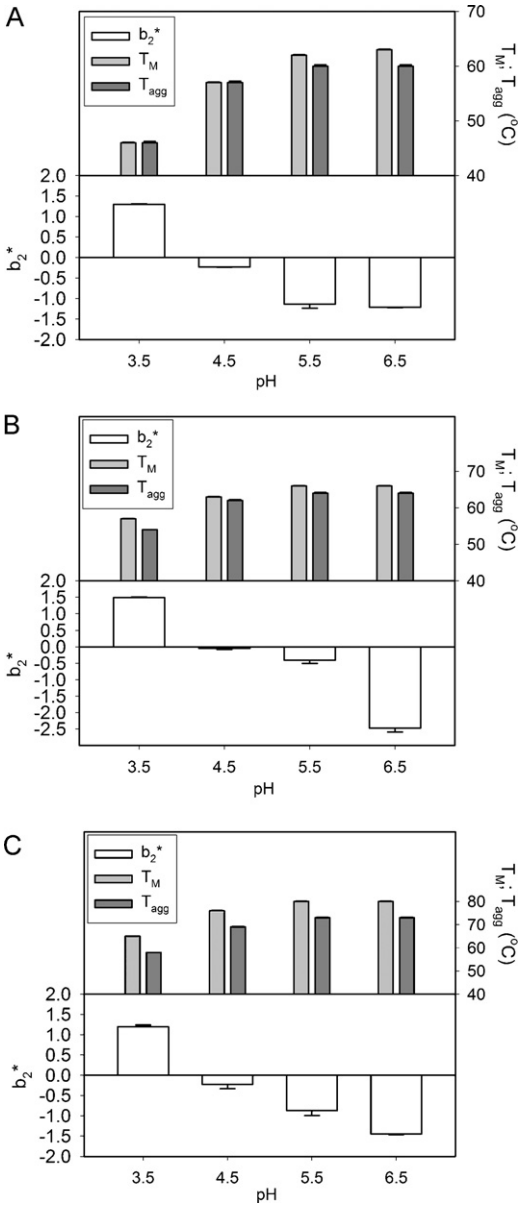

Fig. 6. Comparison of T_M, T_{agg} (defined in text), and b_2^* for three IgG1 antibodies as a function of pH (data from Sahin et al. (2010)). Panel (A) is the same antibody as in Fig. 2 (denoted IgG1.4 in Sahin et al. (2010)), while (B) and (C) differ from (A) in their complementary-determining regions (denoted IgG1.1 and IgG1.3 in Sahin et al. (2010)). T_M values are those for the largest endotherm from DSC, as this corresponds to unfolding of the most aggregation prone domain(s) for this protein (cf., Fig. 2).

T_M, with higher T_M hopefully correlating with lower k_{obs} for a given choice of formulation and sample temperature (Remmele et al., 1998). Fig. 6 provides an example for which T_M is reasonably predictive of relative aggregation rates. In this case, T_M and the storage temperature (T_{agg}) at which $1/k_{obs} \sim 1$ h correlate well—increasing T_M by increasing pH corresponds to increasing T_{agg}. However, as a counter-example Fig. 7 shows a comparison of T_M and k_{obs} (at 50 °C) for wild-type (WT) gamma-D crystallin and two of its point mutations (S130P and M69Q) at a common set of solution conditions. In this case, both point mutants have much lower k_{obs} than WT, but this corresponds to an increase in T_M for only M69Q. Surprisingly, S130P is clearly the most stable in terms of k_{obs}, but has a T_M much lower than that for WT or M69Q. Together, Figs. 6 and 7 illustrate that although T_M may influence aggregation rates, it is at best reflective of only one contribution to k_{obs} – i.e., the contribution from monomer conformational stability. These examples and

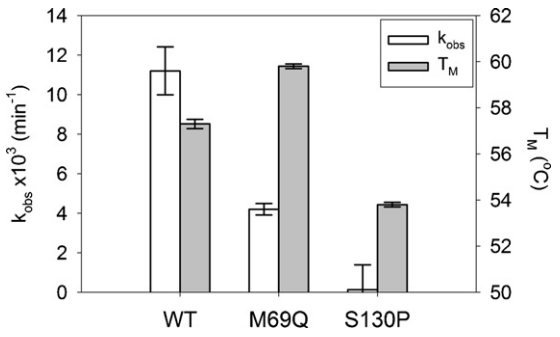

Fig. 7. Comparison of T_M and k_{obs} (50 °C) for wild-type (WT) and two point-mutants (M69Q and S130P) for γ-D crystallin that were designed to differentially effect aggregation rates via enchanced conformational stability or disruption of aggregation "hot spots" in the sequence, respectively (data from Sahin et al. (2011)).

the discussion in Sec. 2 regarding difficulties in predicting *a priori* which T_M for multi-domain proteins corresponds to unfolding of the most aggregation-prone domain(s) help to highlight the limitations of purely T_M-based approaches for predicting aggregation rates, or even qualitatively ranking of relative rates.

5.2. Structure-based predictions and relative aggregation rates

As the discussion in Sec. 4 highlighted, structure-based predictors provide a possible means to rank mutations for a given protein that are likely to result in an increase or decrease in the intrinsic aggregation propensity, but the calculators assume that aggregation prone sequences are solvent exposed and available to interact strongly with another protein. Trout and co-workers (Chennamsetty et al., 2010) showed this could be a useful way to rank different mutants' relative aggregation propensity, provided that the aggregation-prone region(s) are primarily hydrophobic and structurally dynamic to be exposed on short time scales. In contrast, most of the multi-variate statistical "aggregation calculators" do not account for tertiary or secondary structure. With the exception of the discussion below regarding interpolating aggregation rates, structure-based predictions provide only qualitative predictions of relative aggregation rates, as the local structure/sequence for a given monomer does not provide direct information on aggregation rates per se.

5.3. B_{22}, Z^*, and relative aggregation rates

The discussion in Sec. 3 illustrated the conceptual link between colloidal protein interactions and k_{obs}, in that more repulsive interactions (large positive b_2^* values and/or large absolute values of Z^*) are expected to lead to lower aggregation rates. Examples exist that appear to support (Chi et al., 2003b) or contradict (Bajaj et al., 2006; Sahin et al., 2010) this reasoning. Fig. 6 provides an example where aggregation rates increase with increasing b_2^*, rather than the expected behavior. Additional results from that study (Sahin et al., 2010) indicated that at the highest pH conditions, electrostatics provided attractive interactions in some cases, yet aggregation was slowest at those pH values. Although Z^* was not determined in that case, the discussion in Sec. 3 highlighted that net charge alone cannot explain or predict attractive colloidal interactions, and thus neither Z^* nor b_2^* would be considered good indicators of relative aggregation rates for this case.

However, the results in Fig. 6 should not be used to dismiss b_2^* and/or Z^*altogether as potentially useful indicators in some respects regarding aggregation. It is helpful to recall that in order to change b_2^* and/or Z^*, even if one does not consider changes in protein sequence, this requires changes in solvent conditions. Fig. 6 and the discussion earlier in this section illustrate that changing pH resulting in changes in both b_2^* and T_M values – and these changed in opposing directions in that example. Furthermore, b_2^* changing from positive to negative was found to be a good indicator of the change from soluble aggregates to large, insoluble particles (Li et al., 2010; Sahin et al., 2010). Although the latter also corresponded with slower aggregation rates, this was likely a result of the increased T_M values—i.e., lower concentrations of (partially) unfolded monomers available to aggregate in the first place.

Thus, it is advisable to consider multiple potential predictors of relative aggregation rates whenever possible. As Figs. 6 and 7 highlight, the difficulty then becomes how to interpret the predictions when they conflict with one another. It is not surprising based on Fig. 1 that changes in formulation or protein sequence can affect more than one stage of aggregation simultaneously. Mechanistic mathematical models exist that attempt to provide frameworks for quantitatively combining the effects of some or all of the stages in Fig. 1 (Andrews and Roberts, 2007; Li and Roberts, 2009; Pallitto and Murphy, 2001; Lee et al., 2007b; Kendrick et al., 1998), but none have yet been successful in predicting rates based purely on biophysical parameters such as T_M, b_2^*, Z^*, or analogous quantities. At the very least this follows because none of these physical quantities captures the essential dynamics or time scale(s) that govern the rate-limiting step(s). This is perhaps the crux of why none of the approaches described thus far in this review provides more than qualitative predictions or rankings for aggregation rates. Stated in another way: if one wishes to predict aggregation rates, one currently needs to measure aggregation rates and use that information as a key input to the predictions. This is a key principle that underlies the approaches in the next sub-section.

5.4. Extrapolation or interpolation to give quantitative rate predictions

Quantitative rate predictions, to date, require either extrapolation or interpolation of measured aggregation rates over a range of T, p, and/or solvent composition. Fundamentally, this is perhaps not surprising because it is currently not possible to experimentally monitor or theoretically predict the rate coefficient(s) or characteristic time scale(s) for the rate-limiting step(s) for aggregation. Therefore any measured aggregation rates inevitably include contributions from multiple steps simultaneously. With the exception of the "aggregation calculators", all of the approaches and models discussed above are focused essentially on the reversible (if not pre-equilibrated) processes of monomer unfolding and self-association (Weiss et al., 2009), or on the thermodynamic favorability of aggregate phase separation (Brummitt et al., 2011b; Li et al., 2010; Sahin et al., 2010). Therefore, none of the approaches earlier in this article are able to provide a quantitative, predicted rate—i.e., an actual number for k_{obs} or an analogous quantity. One requires experimental rate data to provide the information – even if only indirectly – regarding the inherent or intrinsic kinetics of aggregation; thus the need for interpolation or extrapolation of experimental rates, even when used as part of mechanistic model (see below).

The structure-based methods that underlie the "aggregation calculators" in Sec. 4 do not include or assess the actual kinetic process of creating a nucleus or subsequent growth via monomer addition or aggregate–aggregate association. Rather, they focus on multivariate statistical models that are regressed to existing database(s) for experimental aggregation rates. The underlying models range in complexity, spanning from simple sequence-property correlators to those based on peptide-docking. Many do not provide rates at all; those that do provide rates are able to do so by interpolating the experimental rate data. Such an approach can, in principle, provide quantitative predictions of aggregation rates if the conditions of interest (protein sequence/structure, T, p, and solvent composition) are similar to those of the experimental database against

which a given "calculator" was regressed to set its model parameters. Unfortunately, the existing databases on peptide aggregation against which current public-domain calculators have been "calibrated" include only a relatively small range of T, p, and solvent composition (Caflisch, 2006; Weiss et al., 2009). This is in addition to the limitations noted in Sec 4 regarding the neglect of conformational changes required to expose "hot spots" for aggregation, and the fact that the databases typically are based on experiments limited to the detection of only amyloid aggregates and/or only insoluble (visible) aggregates. As such, it remains an outstanding challenge to accurately predict aggregation rates of foldable proteins based on just the predictions from available "aggregation calculators".

The discussion of "aggregation calculators" not withstanding, any approach that involves interpolating experimental aggregation kinetics will constrain one to lie within the range of sample conditions and time scales that are experimentally convenient (Li et al., 2010). Given that target product shelf lives are typically multi-year, while product development decisions and choices of product composition typically must be made on much shorter time scales, extrapolation of shorter-time or "accelerated" aggregation rates becomes inevitable to some degree.

Extrapolation approaches can be roughly grouped into three categories: empirical, phenomenological, and mechanistic. Empirical approaches assume a simple, mathematically convenient dependence of k_{obs} on the physical parameters of interest, such as pH, excipient concentration(s), and temperature. A common but relatively simple example of an empirical extrapolation is to use statistical design of experiments and/or multi-variate regression to fit experimental k_{obs} values to an empirical (often linear or polynomial) function of the formulation variables of interest (Li et al., 2010; Bai et al., 2003). One can then empirically extrapolate to ranges of formulation conditions outside the data set used to regress the model parameters. Unfortunately, such extrapolations are often inaccurate because k_{obs} depends in a non-linear or otherwise complex manner on variables such as temperature, pH, protein concentration, and excipient concentration(s) (Li et al., 2010; Cleland et al., 1993; Wang, 2005).

Phenomenological extrapolation approaches are based on a physical model that may be oversimplified, but at least provides a rational functional form for the extrapolation. Perhaps the most common example is Arrhenius extrapolation of higher-T, accelerated rate data to lower-T, "real-time" storage conditions (Yoshioka et al., 1994). Based on the idea of a single activated step controlling the observed rate of aggregation, one would expect $\ln k_{obs}$ to scale linearly with the inverse of the absolute temperature—i.e., so-called Arrhenius behavior. If this approximation holds, then an Arrhenius extrapolation may be sufficiently accurate to provide reasonable predictions for k_{obs} (Yoshioka et al., 1994). Even with a more complex aggregation mechanism, Arrhenius behavior may be observed if one is only considering a relatively small range of temperatures, particularly if one is able to focus on a relatively small extrapolation from a base set of conditions that are already well characterized (Weiss et al., 2009). In general, a phenomenological extrapolation is preferred over an empirical one, although both may be insufficient to provide accurate predictions of k_{obs} (Roberts et al., 2003; Cleland et al., 1993; Perico et al., 2009).

In general, a mechanistic extrapolation will likely be needed if k_{obs} depends on temperature, protein sequence, and/or formulation variables in a complex (i.e., "nonlinear") manner. From a mechanistic perspective, the two most likely reasons for such complex behavior of k_{obs} are: (1) the rate-limiting step or key steps in the mechanism of aggregation changes as a function of whatever variable is being extrapolated (Perico et al., 2009); (2) one or more of the key steps in aggregation may intrinsically have a strongly non-linear dependence on the extrapolating variable. A simple example of (1) is a case in which aggregation proceeds through a chemically altered intermediate under some conditions but not others; for example, if disulfide shuffling or chain clipping populates the dominant aggregation-prone monomer form(s) at some temperatures but not others (Perico et al., 2009; Rajan et al., 2010). This results in net non-Arrhenius behavior if the competing rate-limiting steps have significantly different activation energies—this may occur even if each of the competing pathways both behave in an effectively Arrhenius manner, because the identity of the rate-limiting step shifts, in this case, as temperature is lowered (Rajan et al., 2010).

An example of (2) is one in which non-Arrhenius behavior occurs because the apparent or effective activation energy includes the enthalpy of unfolding. This is expected on long time scales for any aggregation mechanism that requires some degree of monomer unfolding, because the temperature dependence of ΔG_{un} is determined by ΔH_0 and Δc_p (Becktel and Schellman, 1987). As a result, as one lowers temperature the fraction of monomeric protein that exists in an aggregation-prone (partially or fully unfolded) state is expected to decrease, provided one does not cool so far as to approach a cold-unfolding temperature. However, the magnitude of the relative change in aggregation-prone monomer content will be greater as one cools from near-but-below T_M than it will be if one is cooling at much lower T. For example, cooling by 5 C at T near T_M can decrease aggregation rates by orders of magnitude, while cooling by the same increment at $T \ll T_M$ may result in a much smaller effect (Roberts et al., 2003; Weiss et al., 2009). This behavior is more pronounced, the larger the value of Δc_p for the region(s) of the protein that unfolded in order to facilitate aggregation, and the larger the range of T over which one extrapolates k_{obs} (Weiss et al., 2009; Roberts, 2007; Roberts et al., 2003).

In principle, such non-Arrhenius behavior for k_{obs} can be accurately predicted if one can obtain equilibrium unfolding thermodynamics as function of T, as was done in at least one reported case (Roberts et al., 2003). Unfortunately, in many cases it is not practical to obtain such equilibrium information because aggregation typically convolutes the interpretation of experimental unfolding curves for aggregation-prone proteins (see also, Sec. 2) unless one can work at sufficiently low protein concentrations to suppress aggregation on the time scale of the unfolding experiments (Roberts et al., 2003). Alternatively, one may be able to generate k_{obs} values across a large enough range of T to apply phenomenological or mechanistic models to give quantitative predictions via interpolation (Kayser et al., unpublished; Brummitt et al., unpublished). Thus, while mechanistic approaches can enable more accurate extrapolations to predict aggregation rates, to date they have been used primarily for only *a posteriori* interpretation or justification of the strong dependence of k_{obs} on variables such as temperature, pH, and excipient levels. As such, no method is currently accepted or in common use to quantitatively predict aggregation rates for proteins, and this remains a long-standing challenge in the field.

6. Outstanding challenges

As the discussion in Sec. 5 highlighted, accurate prediction of aggregation rates as a function of protein sequence and/or sample conditions is not yet generally possible in more than a qualitative manner except for select examples (Roberts et al., 2003)—and even from a qualitative perspective there are notable examples where predictions are inaccurate (Bajaj et al., 2006; Sahin et al., 2010, 2011). This section summarizes some of the key technical challenges that must be addressed with current or emerging experimental and/or theoretical approaches, and that may then ultimately lead to improved predictability of aggregation rates.

6.1. Local unfolding & identification of aggregation-prone regions

As the discussion in Sec. 1, 2, and 4 highlighted, aggregation of foldable proteins appears to be driven by strong favorable inter-protein contacts between relatively small stretches of amino acids, and it is often not clear where these stretches actually exist in a given protein. The available "aggregation calculators" make predictions for the location of such sequences, but there are few experimental examples where those predictions have been validated for foldable proteins (Ivanova et al., 2006; Zhang et al., 2010; Sahin et al., 2011). Even if the predicted sequences are correct, there remains the question of whether and how they become exposed and available to interact with sequences on other proteins. For multi-domain proteins, unfolding of a domain per se may not be needed, as simply disrupting the domain–domain interface may be sufficient (Worn and Pluckthun, 2001).

If aggregation is much slower than the conformational dynamics that reveal aggregation-prone sequences for a given protein, then the thermodynamics of unfolding of that region will determine the fraction of monomers in solution that are available, on average, as aggregation-prone or "reactive" species in Fig. 1. Currently, the large majority of available experimental techniques to measure unfolding free energies can do so only in a relatively global sense. That is, they at best provide unfolding free energies for large cooperative units or domains of a protein, or for the entire protein itself (Freire et al., 1992; Worn, 2001; Ionescu et al., 2008; Flaugh et al., 2005a,b). As such, they provide information regarding the relative amount of a given conformational state in a thermodynamic sense, but that state is composed of a statistical ensemble of structures—not all of which may reveal the aggregation-prone sequence(s) to similar degrees.

Potential experimental approaches to probing spatially resolved "local unfolding" in proteins include NMR and/or mass spectrometry coupled with HD exchange as a function of solvent conditions and/or temperature, as well as a range of chemical ligands and/or dyes that maybe more or less sensitive to different types of local conformational changes. To the best of the authors' knowledge, these techniques have not yet been used to monitor or characterize aggregation-prone regions in monomers prior to aggregation, although they have been used for *a posteriori* analysis of aggregate structures to help identify key contacts and infer the location of "hot spots" in the parent monomers (Paravastu et al., 2008; Zhang et al., 2010; Tobler and Fernandez, 2002), and in screening formulation conditions to try to minimize local unfolding (Maas et al., 2007; Demeule et al., 2009; Gabellieri and Strambini, 2006). Computational tools also exist that attempt to predict local unfolding free energies (Hilser et al., 2006), but to the best of the authors' knowledge these have not yet been used to predict or correlate aggregation rates.

6.2. Improved understanding of nucleation mechanisms

The discussion earlier in this section highlighted that no available technique – experimental or computational – has been shown generally to probe the event(s) of nucleation directly. In many cases, experimental aggregation rates are too slow for the rate-limiting step to be either unfolding (stage 1 in Fig. 1) or diffusion of molecules to reach each other as part of reversible self-association (stage 2 in Fig. 1). That is, the characteristic time scales for unfolding or for diffusion of proteins in solution are typically much shorter than storage of times of pharmaceutical interest; in such cases, unfolding and/or reversible self-association steps are expected to pre-equilibrate, and it is the thermodynamics rather than the kinetics of those steps that is more relevant to predicting k_{obs}. A simple test to help locate the rate-limiting step at a qualitative level is the dependence of shelf life or k_{obs} on initial protein concentration (c_0). Unfolding-limiting aggregation requires k_{obs} have little no dependence on c_0, although at high protein concentrations k_{obs} being independent of c_0 can also occur when unfolding is not rate limiting (Roberts, 2007).

Independent of exactly where the rate-limiting step(s) lie in Fig. 1, the key intermediate(s) in the process of nucleation are typically too transient and poorly populated to be isolated or detected directly in experiment. Furthermore, the proteins in question are too large to be viable candidates for probing nucleation in atomistic detail via theory and simulation – current computational capabilities limit such studies to only relatively small polypeptides (Zanuy et al., 2003). Presently, one is often limited experimentally to only indirectly deducing the stoichiometry of the nuclei via the dependence of aggregation rates on protein concentration (Ferrone, 1999; Andrews and Roberts, 2007; Brummitt et al., 2011b; Chi et al., 2003b), and inferring the likely location of key regions that are involved in nucleation via *a posteriori* structural and/or mutational analysis of the "downstream" aggregates as nuclei grow (Zhang et al., 2010; Ignatova et al., 2007). The inability to either measure or theoretically predict the dynamics of the rate-limiting step(s) in nucleation is perhaps the largest hurdle to truly *a priori* prediction of aggregation rates. This is even further complicated if nucleation occurs at the liquid–air or one of the liquid–solid interfaces that therapeutic proteins likely encounter during production, shipping, and storage. Measuring or predicting the effects of surface adsorption on global or local unfolding, as well understanding the role that surfaces plays in nucleating new aggregates in general remains a major outstanding hurdle (see also, next section).

6.3. Aggregation mediated by bulk surfaces

In much of the above discussion, the process of aggregate formation was deliberately not presented with a bias towards whether any or all of the steps in Fig. 1 occur in bulk solution or at liquid–vapor or liquid–solid interfaces. In principle, they can each occur in bulk and at interfaces. However, most of the approaches used to date for predicting aggregation rates implicitly assume bulk solution measurements and quantities are relevant—e.g., T_M and B_{22}. The potential importance of the liquid–solid, liquid–liquid, and/or liquid–vapor interface for protein aggregation is illustrated by the increasing number of empirical or phenomenological studies that show aggregation can be accelerated by using agitation to entrain air (Kiese et al., 2008) or to increase exposure to solid–liquid interfaces (Biddlecombe et al., 2007; Jiang et al., 2009), as well by spiking with solid materials (Bee et al., 2009; Jiang et al., 2009) or insoluble liquids (Thirumangalathu et al., 2009), and that these effects can be mitigated by addition of surfactants that presumably compete for at least some of those same interfaces (Wang, 2005).

However, the mechanism(s) for surface-mediated aggregation are even less well understood than those for bulk aggregate formation. At a qualitative level, it may be reasonable to assume that surface-mediated aggregation will involve some or all of the steps in Fig. 1, combined with additional steps for transport of proteins to/from the surface. Even if this is the case, prediction of aggregation rates remains hampered for a number of reasons. One of which is the practical question of how to design bench-scale accelerated stability experiments that provide a surface-mediated driving force for aggregation that is similar to that experienced by proteins during manufacture, shipping, and/or storage—e.g., including considerations such as ratios of head-space to liquid volume, surface area to total volume ratio, total container surface contact of the liquid, and the chemistry and/or roughness of the surface (Kiese et al., 2008; Biddlecombe et al., 2007).

Another is the experimental challenge of monitoring the conformational state and/or oligomerization state(s) of proteins at the interface between two phases. Experimentally, there are very

few available techniques that can unambiguously probe the conformational state(s) and/or spatial arrangements of proteins at solid–liquid and vapor–liquid interfaces. From a theoretical perspective, simulating just the equilibrium adsorption of even small peptides at the bulk interface between two phases is itself a challenge if one is interested in molecular details (Miller et al., 2009). Similarly, it is computationally challenging to simulate just the self-association of folded proteins at the interface of two-phase systems (Choutko et al., 2011); extending this to two or more dynamically flexible proteins undergoing unfolding and aggregation simultaneously is presently untenable with conventional approaches. Given that it is currently unknown where the rate-limiting step(s) lie for surface-mediated aggregation, accurate prediction of aggregation rates in such cases will first require further advances in the community's understanding of the underlying mechanisms compared to the seemingly simpler case of bulk aggregation.

6.4. Aggregation and self-association for proteins at high concentrations

The past decade or so has seen a dramatic increase in the number of monoclonal antibody (MAb) or derivative candidates in product development (Reichert et al., 2005). Often, these molecules can achieve rather high solubilities (>100 g L^{-1}) and require relatively high doses (~mg kg^{-1}) to be clinically effective. These factors, combined with a practical need to deliver subcutaneous doses for chronic indications with volumes of no more than approximately 1 mL for each injection, leads to many potential products being developed at much higher concentrations (~10^2 g L^{-1}) than was historically the case. This poses a number of challenges from the perspective of predicting aggregation rates.

At a minimum, there are the practical constraints of available experimental assays for monitoring aggregation. The large majority of analytical tools were developed over the latter half of the twentieth century, with a view towards use with much lower protein concentrations (~1 g L^{-1} or below). This is potentially problematic because commercially available instruments then require samples to be diluted many fold before they can be assayed, and dilution may then drive "weakly bound" aggregates, if present, to dissociate before they can be detected and characterized. If one is concerned with only net-irreversible aggregates, then the question of dilution is less of a concern from the standpoint of monitoring the rates of aggregation.

However, if one is seeking to predict aggregation rates via mechanistic approaches focused on unfolding and protein–protein interactions (cf. Sec. 2 and 3) then this may again be problematic because so-called crowding effects become important for folding and self-association thermodynamics and dynamics at high protein concentrations (Zhou et al., 2008), as well as the fact that the proteins themselves can become the dominant (and highly multivalent) counter-ion species (Gokarn et al., 2008). In practical terms, this means that values of biophysical properties such as T_M, B_{22}, and Z^* measured at low concentrations may not be useful as predictive tools at much higher concentrations, and it would be beneficial to have experimental approaches to measure changes in conformational stability and protein–protein interactions in high-concentration protein solutions. The former will likely prove to remain problematic, as measuring unfolding thermodynamics is problematic at high concentrations because of the competition between refolding and aggregation that greatly favors aggregation as concentration is increased (Privalov and Potekhin, 1986; Roberts et al., 2003). The latter may be achievable with available scattering techniques that are not limited to only dilute conditions (Velev et al., 1998; Minton, 2007; Fernandez and Minton, 2009; Blanco et al., in preparation), but presently such techniques are not in wide-spread use. Some of the spectroscopic techniques such as IR, Raman, and NMR are suitable for high concentration assays, however, as discussed earlier, these may not have adequate sensitivity to detect small fractions of non-native species.

6.5. Improved means to determine accelerated aggregation rates

Finally, if one adopts the philosophy that aggregation rates are most effectively predicted by rationally extrapolating from accelerated conditions – independent of whether an empirical, phenomenological, or mechanistic extrapolation is employed – then there are number of outstanding challenges for practical predictions that follow from the discussions above. The first is the question of what kind of accelerated method does one employ, and what accelerating variable(s) are most predictive. For example, should one heat to accelerate aggregation, and if so what is the relevant temperature range in order to be predictive? Should one instead agitate solutions to accelerate aggregation, and if so what mechanical configuration should be used—e.g., shaking vs. vortexing vs. sparging, etc.? There is currently no consensus in the community, and no unambiguous examples from which to draw general answers to these important questions. It is generally recognized however, that because proteins aggregate through various routes depending on the applied stress, one needs a series of accelerated conditions to attempt to predict different types of aggregation pathways relevant to producing a stable, safe and efficacious dosage form. Of course, these questions are intimately tied to understanding the mechanisms of aggregation – as the field continues to progress in those areas, so too will our ability to better design predictive experiments.

7. Summary

Control of aggregation rates is a common challenge during development of protein-based pharmaceuticals and other biotechnology products. Most current approaches can be grouped into a number of categories depending on whether they focus primarily on: (i) unfolding and higher-order-structure perturbations, (ii) reversible self-association, (iii) intrinsic "hot spots" or aggregation propensity of the polypeptide sequence and structure, or (iv) rational interpolation or extrapolation of accelerated aggregation rates. Approaches (i) to (iii) are more directly tied to the current understanding or assumptions regarding the mechanisms of aggregation, but are limited in their ability to provide more than qualitative predictions. Approaches in category (iv) naturally provide quantitative predictions but the accuracy of those predictions often relies heavily on the underlying mechanistic understanding. As such, it is likely that approaches that combine features of all of the above will prove most lucrative in the near term. Truly *a priori* predictions will likely remain an unanswered challenge until the process of nucleation is directly accessible for study at a molecular level in both experiment and theory/simulation.

Fig. 8 provides an overview and summary of the approaches reviewed here, along with their qualitative vs. (semi-)quantitative relationship to aggregation rates, as well as rough estimates regarding relative resource/time/material requirements (including computational burden). Rather than argue that there is an optimal choice or recipe of how to combine the different approaches in a standardized platform, it is important to highlight that aggregation studies serve multiple purposes during the development of protein products, and these purposes differ depending on the stage one considers within the development process—e.g., due to limitations of material and/or other resources, different needs of clinical development, and different regulatory requirements at different stages (Weinberg et al., 2010). As such, the pros and cons of each approach should be weighed; a suitable combination of the avail-

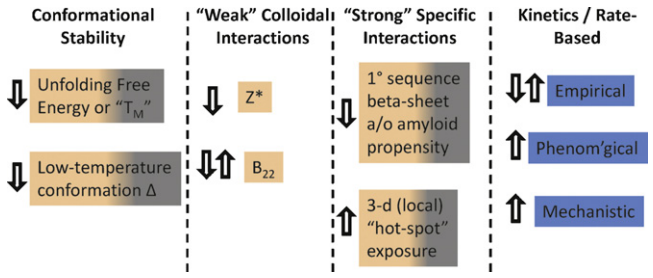

Fig. 8. Schematic overview of the major approaches reviewed here. Color coding summarizes whether approaches in a given category tend to be qualitative (gray), semi-quantitative (orange/red), or quantitative (blue) in terms of the relationship between the measured or predicted quantities and aggregation rates. The arrows indicate relatively high (up arrow) or low (down arrow) time, resource, and/or expense associated with the given approach. Cases where more than one arrow or color occur are those in which some methods are more or less in these categories. (For interpretation of the references to color in this figure legend, the reader is referred to the web version of the article.)

able approaches is advisable to ensure an acceptable product, based on a balance between quantitative accuracy, the time-frame(s) on which aggregation rate predictions are needed, and the availability of resources and material.

There are a number of additional outstanding challenges for the community regarding mechanistic understanding of aggregation so as to enable more accurate rate predictions. These include better experimental and theoretical tools: to probe local unfolding and identify aggregation-prone regions that may become solvent exposed only transiently and infrequently; to work with high-concentration solutions where many current assays are not directly viable; to treat the process of aggregation mediated by liquid–solid, liquid–liquid, and/or liquid/vapor interfaces; and to design the most relevant and predictive accelerated stability studies. Although robust prediction of aggregation rates remains an outstanding challenge in the field, it also remains an area of active research, and one that will continue to benefit from both fundamental and applied science and engineering spanning across a number of fields.

Role of funding source

Pfizer, Inc. funded, in part, the composition of this report, and was involved in the design or composition of this review, or the interpretation of the data only via the involvement of the author(s) of the report. Prior to submission, the sponsor was required to review the report for any intellectual property conflicts.

Acknowledgements

Pfizer, Inc. is gratefully acknowledged for financial support, and Prof. B. Trout is thanked for providing a copy of Kayser et al. ahead of publication.

References

Alford, J.R., Kendrick, B.S., Carpenter, J.F., Randolph, T.W., 2008. Measurement of the second osmotic virial coefficient for protein solutions exhibiting monomer-dimer equilibrium. Anal. Biochem. 377, 128–133.
Andrews, J.M., Roberts, C.J., 2007. A Lumry-Eyring nucleated polymerization model of protein aggregation kinetics: 1. Aggregation with pre-equilibrated unfolding. J. Phys. Chem. B 111, 7897–7913.
Azriel, R., Gazit, E., 2001. Analysis of the minimal amyloid-forming fragment of the islet amyloid polypeptide. J. Biol. Chem. 276, 34156–34161.
Bai, S.J., Katayama, D.S., Chou, D.K.C., Anchordoquy, T.J., Nayar, R., Manning, M.C., 2003. High-throughput formulation of biopharmaceutical products in the postgenomic age. Am. Biotech. Lab. 21, 28F–128F.
Bajaj, H., Sharma, V.K., Badkar, A., Zeng, D., Nema, S., Kalonia, D.S., 2006. Protein structural conformation and not second virial coefficient relates to long-term irreversible aggregation of a monoclonal antibody and ovalbumin in solution. Pharm. Res. 23, 1382–1394.
Becktel, W.J., Schellman, J.A., 1987. Protein stability curves. Biopolymers 26, 1859–1877.
Bee, J.S., Nelson, S.A., Freund, E., Carpenter, J.F., Randolph, T.W., 2009. Precipitation of a monoclonal antibody by soluble tungsten. J. Pharm. Sci. 98, 3290–3301.
Ben Naim, A., 1992. Statistical Thermodynamics for Chemists and Biochemists. Plenum press, New York.
Biddlecombe, J.G., Craig, A.V., Zhang, H., Uddin, S., Mulot, S., Fish, B.C., Bracewell, D.G., 2007. Determining antibody stability: creation of solid-liquid interfacial effects within a high shear environment. Biotechnol. Prog. 23, 1218–1222.
Brummitt, R.K., Nesta, D.P., Chang, L., Chase, S.F., Laue, T.M., Roberts, C.J., 2011a. Non-native aggregation of an IgG1 antibody in acidic conditions: 1. Unfolding, colloidal interactions, and formation of high molecular weight aggregates. J. Pharm. Sci. 100, 2087–2103 (Early View).
Brummitt, R.K., Nesta, D.P., Chang, L., Kroetsch, A.M., Roberts, C.J., 2011b. Non-native aggregation of an igg1 antibody in acidic conditions: 2. Nucleation-and-growth kinetics with competing growth mechanisms. J. Pharm. Sci. 100, 2104–2119 (Early View).
Caflisch, A., 2006. Computational models for the prediction of polypeptide aggregation propensity. Curr. Opin. Chem. Biol. 10, 437–444.
Cellmer, T., Bratko, D., Prausnitz, J.M., Blanch, H.W., 2007. Protein aggregation in silico. Trends Biotechnol. 25, 254–261.
Chase, S.F., Laue, T.M., 2008. The determination of protein valence by capillary electrophoresis. Beckman Coulter P/ACE Setter 12 (1).
Chennamsetty, N., Voynov, V., Kayser, V., Helk, B., Trout, B.L., 2010. Prediction of aggregation prone regions of therapeutic proteins. J. Phys. Chem. B 114, 6614–6624.
Chennamsetty, N., Helk, B., Voynov, V., Kayser, V., Trout, B.L., 2009. Aggregation-prone motifs in human immunoglobulin G. J. Mol. Biol. 391, 404–413.
Chi, E.Y., Krishnan, S., Randolph, T.W., Carpenter, J.F., 2003a. Physical stability of proteins in aqueous solution: mechanism and driving forces in nonnative protein aggregation. Pharm. Res. 20, 1325–1336.
Chi, E.Y., Krishnan, S., Kendrick, B.S., Chang, B.S., Carpenter, J.F., Randolph, T.W., 2003b. Roles of conformational stability and colloidal stability in the aggregation of recombinant human granulocyte colony-stimulating factor. Protein Sci. 12, 903–913.
Chiti, F., Dobson, C.M., 2006. Protein misfolding, functional amyloid, and human disease. Annu. Rev. Biochem. 75, 333–366.
Choutko, A., Glattli, A., Fernandez, C., Hilty, C., Wuthrich, K., Gunsteren, W.F., 2011. Membrane protein dynamics in different environments: simulation study of the outer membrane protein X in a lipid bilayer and in a micelle. Eur. Biophys. J. 40, 39–58.
Cleland, J.L., Powell, M.F., Shire, S.J., 1993. The development of stable protein formulations: a close look at protein aggregation, deamidation, and oxidation. Crit. Rev. Ther. Drug Carrier Syst. 10, 307–377.
Conchillo-Sole, O., de, G., Aviles, F.X., Vendrell, J., Daura, X., Ventura, S., 2007. AGGRESCAN: a server for the prediction and evaluation of "hot spots" of aggregation in polypeptides. BMC Bioinf. 8.
Das, T., Nema, S., 2008. Protein particulate issues in biologics development. Am. Pharm. Rev. 11 (52), 54–57.
Demeule, B., Palais, C., Machaidze, G., Gurny, R., Arvinte, T., 2009. New methods allowing the detection of protein aggregates: a case study on trastuzumab. MAbs 1, 142–150.
Eisenberg, D., Nelson, R., Sawaya, M.R., Balbirnie, M., Sambashivan, S., Ivanova, M.I., Madsen, A.O., Riekel, C., 2006. The structural biology of protein aggregation diseases: fundamental questions and some answers. Acc. Chem. Res. 39, 568–575.
Fändrich, M., Fletcher, M.A., Dobson, C.M., 2001. Amyloid fibrils from muscle myoglobin. Nature 410, 165–166.
Fernandez, C., Minton, A.P., 2009. Static light scattering from concentrated protein solutions II: experimental test of theory for protein mixtures and weakly self-associating proteins. Biophys. J. 96, 1992–1998.
Fernandez-Escamilla, A., Rousseau, F., Schymkowitz, J., Serrano, L., 2004. Prediction of sequence-dependent and mutational effects on the aggregation of peptides and proteins. Nat. Biotechnol. 22, 1302–1306.
Ferrone, F., 1999. Analysis of protein aggregation kinetics. Methods Enzymol. 309, 256–274.
Filipe, V., Hawe, A., Schellekens, H., Jiskoot, W., 2010. Aggregation and immunogenicity of therapeutic proteins. In: Aggregation Ther. Proteins. John Wiley & Sons, Inc., pp. 403–433, 1 plate.
Flaugh, S.L., Kosinski-Collins, M.S., King, J., 2005a. Interdomain side-chain interactions in human γD crystallin influencing folding and stability. Protein Sci. 14, 2030–2043.
Flaugh, S.L., Kosinski-Collins, M.S., King, J., 2005b. Contributions of hydrophobic domain interface interactions to the folding and stability of human γD-crystallin. Protein Sci. 14, 569–581.
Freire, E., Murphy, K.P., Sanchez-Ruiz, J.M., Galisteo, M.L., Privalov, P.L., 1992. The molecular basis of cooperativity in protein folding. Thermodynamic dissection of interdomain interactions in phosphoglycerate kinase. Biochemistry 31, 250–256.
Gabellieri, E., Strambini, G.B., 2006. ANS fluorescence detects widespread perturbations of protein tertiary structure in ice. Biophys. J. 90, 3239–3245.
Gabrielson, J.P., Brader, M.L., Pekar, A.H., Mathis, K.B., Winter, G., Carpenter, J.F., Randolph, T.W., 2006. Quantitation of aggregate levels in a recombinant humanized monoclonal antibody formulation by size-exclusion chromatography, asymmetrical flow field flow fractionation, and sedimentation velocity. J. Pharm. Sci. 96, 268–279.

Goetz, H., Kuschel, M., Wulff, T., Sauber, C., Miller, C., Fisher, S., Woodward, C., 2004. Comparison of selected analytical techniques for protein sizing, quantitation and molecular weight determination. J. Biochem. Biophys. Methods 60, 281–293.
Gokarn, Y.R., Kras, E., Nodgaard, C., Dharmavaram, V., Fesinmeyer, R.M., Hultgen, H., Brych, S., Remmele, R.L., Brems, D.N., Hershenson, S., 2008. Self-buffering antibody formulations. J. Pharm. Sci. 97, 3051–3066.
He, F., Phan, D.H., Hogan, S., Bailey, R., Becker, G.W., Narhi, L.O., Razinkov, V.I., 2010. Detection of IgG aggregation by a high throughput method based on extrinsic fluorescence. J. Pharm. Sci. 99, 2598–2608.
Hilser, V.J., Garcia-Moreno, E., Oas, T.G., Kapp, G., Whitten, S.T., 2006. A statistical thermodynamic model of the protein ensemble. Chem. Rev. (Washington, DC, USA) 106, 1545–1558.
Ignatova, Z., Thakur, A.K., Wetzel, R., Gierasch, L.M., 2007. In-cell aggregation of a polyglutamine-containing chimera is a multistep process initiated by the flanking sequence. J. Biol. Chem. 282, 36736–36743.
Ionescu, R.M., Vlasak, J., Price, C., Kirchmeier, M., 2008. Contribution of variable domains to the stability of humanized IgG1 monoclonal antibodies. J. Pharm. Sci. 97, 1414–1426.
Israelachvili, J.N., 1991. Intermolecular and Surface Forces. McGraw-Hill Publishing Co., Japan, Ltd.
Ivanova, M.I., Thompson, M.J., Eisenberg, D., 2006. A systematic screen of β2-microglobulin and insulin for amyloid-like segments. Proc. Natl. Acad. Sci. U.S.A. 103, 4079–4082.
Jaroniec, C.P., MacPhee, C.E., Astrof, N.S., Dobson, C.M., Griffin, R.G., 2002. Molecular conformation of a peptide fragment of transthyretin in an amyloid fibril. Proc. Natl. Acad. Sci. U.S.A. 99, 16748–16753.
Jiang, Y., Nashed-Samuel, Y., Li, C., Liu, W., Pollastrini, J., Mallard, D., Wen, Z., Fujimori, K., Pallitto, M., Donahue, L., Chu, G., Torraca, G., Vance, A., Mire-Sluis, T., Freund, E., Davis, J., Narhi, L., 2009. Tungsten-induced protein aggregation: solution behavior. J. Pharm. Sci. 98, 4695–4710.
Jin, L., Yu, Y., Gao, G., 2006. A molecular-thermodynamic model for the interactions between globular proteins in aqueous solutions: applications to bovine serum albumin (BSA), lysozyme, α-chymotrypsin, and immuno-gamma-globulins (IgG) solutions. J. Colloid Interface Sci. 304, 77–83.
Jones, S., Manning, J., Kad, N.M., Radford, S.E., 2003. Amyloid-forming peptides from β2-microglobulin-insights into the mechanism of fibril formation in vitro. J. Mol. Biol. 325, 249–257.
Kendrick, B.S., Cleland, J.L., Lam, X., Nguyen, T., Randolph, T.W., Manning, M.C., Carpenter, J.F., 1998. Aggregation of recombinant human interferon gamma: kinetics and structural transitions. J. Pharm. Sci. 87, 1069–1076.
Kiese, S., Papppenberger, A., Friess, W., Mahler, H., 2008. Shaken, not stirred: mechanical stress testing of an IgG1 antibody. J. Pharm. Sci. 97, 4347–4366.
Laurence, J.S., Middaugh, C.R., 2010. Fundamental structures and behaviors of proteins. In: Aggregation Ther. Proteins. John Wiley & Sons, Inc., pp. 1–61, 2 plates.
Lee, C.C., Walters, R.H., Murphy, R.M., 2007a. Reconsidering the mechanism of polyglutamine peptide aggregation. Biochemistry 46, 12810–12820.
Lee, C., Nayak, A., Sethuraman, A., Belfort, G., McRae, G.J., 2007b. A three-stage kinetic model of amyloid fibrillation. Biophys. J. 92, 3448–3458.
Lepock, J.R., Ritchie, K.P., Kolios, M.C., Rodahl, A.M., Heinz, K.A., Kruuv, J., 1992. Influence of transition rates and scan rate on kinetic simulations of differential scanning calorimetry profiles of reversible and irreversible protein denaturation. Biochemistry 31, 12706–12712.
Li, L., von, B., Mandelkow, E., Mandelkow, E., 2002. Structure, stability, and aggregation of paired helical filaments from tau protein and FTDP-17 mutants probed by tryptophan scanning mutagenesis. J. Biol. Chem. 277, 41390–41400.
Li, Y., Roberts, C.J., 2009. Lumry-Eyring nucleated-polymerization model of protein aggregation kinetics. 2. Competing growth via condensation and chain polymerization. J. Phys. Chem. B 113, 7020–7032.
Li, Y., Ogunnaike, B.A., Roberts, C.J., 2010. Multi-variate approach to global protein aggregation behavior and kinetics: effects of pH, NaCl, and temperature for α-chymotrypsinogen A. J. Pharm. Sci. 99, 645–662.
Liu, J., Andya, J.D., Shire, S.J., 2006. A critical review of analytical ultracentrifugation and field flow fractionation methods for measuring protein aggregation. AAPS J. 8, E580–E589.
Maas, C., Hermeling, S., Bouma, B., Jiskoot, W., Gebbink, M.F.B.G., 2007. A role for protein misfolding in immunogenicity of biopharmaceuticals. J. Biol. Chem. 282, 2229–2236.
Mahler, H., Friess, W., Grauschopf, U., Kiese, S., 2009. Protein aggregation: pathways, induction factors and analysis. J. Pharm. Sci. 98, 2909–2934.
Marky, L.A., Breslauer, K.J., 1987. Calculating thermodynamic data for transitions of any molecularity from equilibrium melting curves. Biopolymers 26, 1601–1620.
McQuarrie, D.A., 1976. Statistical Mechanics. Harper and Row.
Miller, C.A., Abbott, N.L., de Pablo, J.J., 2009. Surface activity of amphiphilic helical β-peptides from molecular dynamics simulation. Langmuir 25, 2811–2823.
Minton, A.P., 2008. Effective hard particle model for the osmotic pressure of highly concentrated binary protein solutions. Biophys. J. 94, L57–L59.
Minton, A.P., 2007. Static light scattering from concentrated protein solutions. I: general theory for protein mixtures and application to self-associating proteins. Biophys. J. 93, 1321–1328.
Morra, G., Meli, M., Colombo, G., 2008. Molecular dynamics simulations of proteins and peptides: from folding to drug design. Curr. Protein Pept. Sci. 9, 181–196.
Morris, A.M., Watzky, M.A., Agar, J.N., Finke, R.G., 2008. Fitting neurological protein aggregation kinetic data via a 2-step, Minimal/"Ockham's Razor" Model: the Finke-Watzky mechanism of nucleation followed by autocatalytic surface growth. Biochemistry 47, 2413–2427.
Neal, B.L., Asthagiri, D., Lenhoff, A.M., 1998. Molecular origins of osmotic second virial coefficients of proteins. Biophys. J. 75, 2469–2477.
Nelson, R., Sawaya, M.R., Balbirnie, M., Madsen, A.O., Riekel, C., Grothe, R., Eisenberg, D., 2005. Structure of the cross-β spine of amyloid-like fibrils. Nature (London, UK) 435, 773–778.
Palaninathan, S.K., Mohamedmohaideen, N.N., Snee, W.C., Kelly, J.W., Sacchettini, J.C., 2008. Structural insight into pH-induced conformational changes within the native human transthyretin tetramer. J. Mol. Biol. 382, 1157–1167.
Pallitto, M.M., Murphy, R.M., 2001. A mathematical model of the kinetics of β-amyloid fibril growth from the denatured state. Biophys. J. 81, 1805–1822.
Paravastu, A.K., Leapman, R.D., Yau, W., Tycko, R., 2008. Molecular structural basis for polymorphism in Alzheimer's β-amyloid fibrils. Proc. Natl. Acad. Sci. U.S.A. 105, 18349–18354, S18349/1-S18349/14.
Perico, N., Purtell, J., Dillon, T.M., Ricci, M.S., 2009. Conformational implications of an inversed pH-dependent antibody aggregation. J. Pharm. Sci. 98, 3031–3042.
Pertinhez, T.A., Bouchard, M., Tomlinson, E.J., Wain, R., Ferguson, S.J., Dobson, C.M., Smith, L.J., 2001. Amyloid fibril formation by a helical cytochrome. FEBS Lett. 495, 184–186.
Picotti, P., De Franceschi, G., Frare, E., Spolaore, B., Zambonin, M., Chiti, F., de Laureto, P.P., Fontana, A., 2007. Amyloid fibril formation and disaggregation of fragment 1-29 of apomyoglobin: insights into the effect of pH on protein fibrillogenesis. J. Mol. Biol. 367, 1237–1245.
Privalov, P.L., 1979. Stability of proteins. Small globular proteins. Adv. Protein Chem. 33, 167–241.
Privalov, P.L., 1982. Stability of proteins. Proteins which do not present a single cooperative system. Adv. Protein Chem. 35, 1–104.
Privalov, P.L., Potekhin, S.A., 1986. Scanning microcalorimetry in studying temperature-induced changes in proteins. Methods Enzymol. 131, 4–51.
Rajan, R.S., Li, T., Arakawa, T., 2010. Case studies involving protein aggregation. In: Aggregation Ther. Proteins. John Wiley & Sons, Inc, pp. 367–401.
Raso, S.W., Abel, J., Barnes, J.M., Maloney, K.M., Pipes, G., Treuheit, M.J., King, J., Brems, D.N., 2005. Aggregation of granulocyte-colony stimulating factor in vitro involves a conformationally altered monomeric state. Protein Sci. 14, 2246–2257.
Rees, D.C., Robertson, A.D., 2001. Some thermodynamic implications for the thermostability of proteins. Protein Sci. 10, 1187–1194.
Reichert, J.M., Rosensweig, C.J., Faden, L.B., Dewitz, M.C., 2005. Monoclonal antibody successes in the clinic. Nat. Biotechnol. 23, 1073–1078.
Remmele, R.L., Nightlinger, N.S., Srinivasan, S., Gombotz, W.R., 1998. Interleukin-1 receptor (IL-1R) liquid formulation development using differential scanning calorimetry. Pharm. Res. 15, 200–208.
Remmele, R.L., Bhat, S.D., Phan, D.H., Gombotz, W.R., 1999. Minimization of recombinant human Flt3 ligand aggregation at the Tm plateau: a matter of thermal reversibility. Biochemistry 38, 5241–5247.
Remmele, R.L., 2005. Microcalorimetric approaches to biopharmaceutical development. In: Anal. Tech. Biopharm. Dev. Marcel Dekker, Inc., pp. 327–381.
Roberts, C.J., Darrington, R.T., Whitley, M.B., 2003. Irreversible aggregation of recombinant bovine granulocyte-colony stimulating factor (bG-CSF) and implications for predicting protein shelf life. J. Pharm. Sci. 92, 1095–1111.
Roberts, C.J., 2007. Non-native protein aggregation kinetics. Biotechnol. Bioeng. 98, 927–938.
Robinson, C.R., Rentzeperis, D., Silva, J.L., Sauer, R.T., 1997. Formation of a denatured dimer limits the thermal stability of Arc repressor. J. Mol. Biol. 273, 692–700.
Rousseau, F., Schymkowitz, J.W.H., Itzhaki, L.S., 2003. The unfolding story of three-dimensional domain swapping. Structure (Cambridge, MA, USA) 11, 243–251.
Sahin, E., Grillo, A.O., Perkins, M.D., Roberts, C.J., 2010. Comparative effects of pH and ionic strength on protein-protein interactions, unfolding, and aggregation for IgG1 antibodies. J. Pharm. Sci. 99, 4830–4848.
Sahin, E., Jordan, J.L., Spatara, M.L., Naranjo, A., Costanzo, J.A., Weiss, W.F., Skaja, R., Fernandez, E.J., Roberts, C.J., 2011. Computational design and biophysical characterization of aggregation-resistant point mutations for γD crystallin illustrate a balance of conformational stability and intrinsic aggregation propensity. Biochemistry, doi:10.1021/bi100978r (available online).
Sanchez, D.G., Pallares, I., Aviles, F.X., Vendrell, J., Ventura, S., 2005. Prediction of "hot spots" of aggregation in disease-linked polypeptides. BMC Struct. Biol. 5.
Sanchez-Ruiz, J.M., Lopez-Lacomba, J.L., Cortijo, M., Mateo, P.L., 1988. Differential scanning calorimetry of the irreversible thermal denaturation of thermolysin. Biochemistry 27, 1648–1652.
Sanchez-Ruiz, J.M., 1992. Theoretical analysis of Lumry-Eyring models in differential scanning calorimetry. Biophys. J. 61, 921–935.
Schellman, J.A., 1997. Temperature, stability, and the hydrophobic interaction. Biophys. J. 73, 2960–2964.
Sharma, V.K., Kalonia, D.S., 2010. Experimental detection and characterization of protein aggregates. In: Aggregation Ther. Proteins. John Wiley & Sons, Inc, pp. 205–256.
Tessier, P.M., Lenhoff, A.M., Sandler, S.I., 2002. Rapid measurement of protein osmotic second virial coefficients by self-interaction chromatography. Biophys. J. 82, 1620–1631.
Thirumangalathu, R., Krishnan, S., Ricci, M.S., Brems, D.N., Randolph, T.W., Carpenter, J.F., 2009. Silicone oil- and agitation-induced aggregation of a monoclonal antibody in aqueous solution. J. Pharm. Sci. 98, 3167–3181.
Timasheff, S.N., 1993. The control of protein stability and association by weak interactions with water: How do solvents affect these processes? Annu. Rev. Biophys. Biomol. Struct. 22, 67–97.

Tobler, S.A., Fernandez, E.J., 2002. Structural features of interferon-γ aggregation revealed by hydrogen exchange. Protein Sci. 11, 1340–1352.
Trovato, A., Seno, F., Tosatto, S.C.E., 2007. The PASTA server for protein aggregation prediction. Protein Eng., Des. Sel. 20, 521–523.
Velev, O.D., Kaler, E.W., Lenhoff, A.M., 1998. Protein interactions in solution characterized by light and neutron scattering: comparison of lysozyme and chymotrypsinogen. Biophys. J. 75, 2682–2697.
Wang, X., Das, T.K., Singh, S.K., Kumar, S., 2009. Potential aggregation prone regions in biotherapeutics: a survey of commercial monoclonal antibodies. MAbs 1, 254–267.
Wang, W., 2005. Protein aggregation and its inhibition in biopharmaceutics. Int. J. Pharm. 289, 1–30.
Wang, W., Roberts, C.J. (Eds.), 2010. Aggregation of Therapeutic Proteins. John Wiley & Sons, Inc..
Weinberg, W.C., Ha, L., Kirschner, S.L., Verthelyi, D.I., 2010. Regulatory perspective on aggregates as a product quality attribute. In: Aggregation Ther. Proteins. John Wiley & Sons, Inc, pp. 435–452.
Weiss, W.F., Hodgdon, T.K., Kaler, E.W., Lenhoff, A.M., Roberts, C.J., 2007. Nonnative protein polymers: structure, morphology, and relation to nucleation and growth. Biophys. J. 93, 4392–4403.
Weiss IV, W.F., Young, T.M., Roberts, C.J., 2009. Principles, approaches, and challenges for predicting protein aggregation rates and shelf life. J. Pharm. Sci. 98, 1246–1277.
Worn, A., Pluckthun, A., 2001. Stability engineering of antibody single-chain Fv fragments. J. Mol. Biol. 305, 989–1010.
Yadav, S., Liu, J., Shire, S.J., Kalonia, D.S., 2010. Specific interactions in high concentration antibody solutions resulting in high viscosity. J. Pharm. Sci. 99, 1152–1168.
Yoshioka, S., Aso, Y., Izutsu, K., Kojima, S., 1994. Is stability prediction possible for protein drugs? Denaturation kinetics of β-galactosidase in solution. Pharm. Res. 11, 1721–1725.
Zanuy, D., Ma, B., Nussinov, R., 2003. Short peptide amyloid organization: stabilities and conformations of the islet amyloid peptide NFGAIL. Biophys. J. 84, 1884–1894.
Zhang, A., Jordan, J.L., Ivanova, M.I., Weiss IV, W.F., Roberts, C.J., Fernandez, E.J., 2010. Molecular level insights into thermally induced α-chymotrypsinogen A amyloid aggregation mechanism and semiflexible protofibril morphology. Biochemistry 49, 10553–10564.
Zhou, H., Rivas, G., Minton, A.P., 2008. Macromolecular crowding and confinement: biochemical, biophysical, and potential physiological consequences. Annu. Rev. Biophys. 37, 375–397.